

See discussions, stats, and author profiles for this publication at: <https://www.researchgate.net/publication/234139136>

# GIS-based landslide susceptibility mapping with probabilistic likelihood ratio and spatial multi-criteria evaluation models (North of Tehran, Iran)

Article in *Arabian Journal of Geosciences* · January 2013

DOI: 10.1007/s12517-012-0825-x

CITATIONS

134

READS

1,474

5 authors, including:



**Hamid Reza Pourghasemi**  
Shiraz University

183 PUBLICATIONS 7,100 CITATIONS

[SEE PROFILE](#)



**Candan Gokceoglu**  
Hacettepe University

238 PUBLICATIONS 9,005 CITATIONS

[SEE PROFILE](#)



**Biswajeet Pradhan**  
University of Technology Sydney

741 PUBLICATIONS 22,828 CITATIONS

[SEE PROFILE](#)

Some of the authors of this publication are also working on these related projects:



Determining soil loss tolerance in calcareous soils of semi-arid regions [View project](#)



Urban Sprawl Assessment [View project](#)

# GIS-based landslide susceptibility mapping with probabilistic likelihood ratio and spatial multi-criteria evaluation models (North of Tehran, Iran)

H. R. Pourghasemi · H. R. Moradi · S. M. Fatemi Aghda · C. Gokceoglu · B. Pradhan

Received: 22 September 2012 / Accepted: 21 December 2012  
© Saudi Society for Geosciences 2013

**Abstract** The aim of this study is to produce landslide susceptibility mapping by probabilistic likelihood ratio (PLR) and spatial multi-criteria evaluation (SMCE) models based on geographic information system (GIS) in the north of Tehran metropolitan, Iran. The landslide locations in the study area were identified by interpretation of aerial photographs, satellite images, and field surveys. In order to generate the necessary factors for the SMCE approach, remote sensing and GIS integrated techniques were applied in the study area. Conditioning factors such as slope degree, slope aspect, altitude, plan curvature, profile curvature, surface area ratio, topographic position index, topographic wetness index, stream power index, slope length, lithology, land use, normalized difference vegetation index, distance from

faults, distance from rivers, distance from roads, and drainage density are used for landslide susceptibility mapping. Of 528 landslide locations, 70 % were used in landslide susceptibility mapping, and the remaining 30 % were used for validation of the maps. Using the above conditioning factors, landslide susceptibility was calculated using SMCE and PLR models, and the results were plotted in ILWIS-GIS. Finally, the two landslide susceptibility maps were validated using receiver operating characteristic curves and seed cell area index methods. The validation results showed that area under the curve for SMCE and PLR models is 76.16 and 80.98 %, respectively. The results obtained in this study also showed that the probabilistic likelihood ratio model performed slightly better than the spatial multi-criteria evaluation. These landslide susceptibility maps can be used for preliminary land use planning and hazard mitigation purpose.

---

H. R. Pourghasemi · H. R. Moradi (✉)  
Department of Watershed Management Engineering, College of Natural Resources and Marine Sciences, Tarbiat Modares University (TMU), Noor, Mazandaran, Iran  
e-mail: hrmoradi1340@yahoo.com

H. R. Moradi  
e-mail: hrmoradi@modares.ac.ir

H. R. Pourghasemi  
e-mail: hamidreza.pourghasemi@yahoo.com

S. M. Fatemi Aghda  
Department of Engineering Geology, Tarbiat Moallem University, Tehran, Iran

C. Gokceoglu  
Applied Geology Division, Department of Geological Engineering, Engineering Faculty, Hacettepe University, Ankara, Turkey

B. Pradhan  
Faculty of Engineering, Department of Civil Engineering, University Putra Malaysia, UPM 43400, Serdang, Selangor, Malaysia

**Keywords** Landslide susceptibility · Spatial multi-criteria evaluation · Frequency ratio · GIS · Tehran metropolitan

## Introduction

The complexity of the earth system's behavior makes it extremely difficult to accurately forecast the future of the earth system, and presents a major challenge to the global change research community (Pielke et al. 2003; Gokceoglu and Sezer 2012). Landslides are a part of the earth surface processes, while considered as one of the most dangerous natural hazards that may follow triggering events (e.g., extreme rainfall and earthquakes) in mountainous areas, causing loss of human life and damage to property (Tien Bui et al. 2012b). Thus, it is necessary to assess landslide susceptibility to facilitate forecasting of this phenomenon. Areas which are predicted as highly susceptible to landslides

are the areas where further slope failure is likely to occur (Althuwaynee et al. 2012). Hence, landslide susceptibility maps rank different sections of land surface according to the degree of actual or potential hazard; thus, planners are able to choose favorable sites for urban and rural development (Parise 2001). In the literature, different approaches have been used to make landslide susceptibility maps. Many studies have evaluated landslide susceptibility using geographic information system (GIS), and many of these studies have utilized probabilistic models (Ozdemir 2009; Yilmaz 2010; Oh and Lee 2010; Oh and Lee 2011; Pourghasemi et al. 2012a, b; Mohammady et al. 2012). Also, statistical analysis is the most frequent method in publications (Aleotti and Chowdhury 1999), including bivariate analysis (e.g., Constantin et al. 2011; Yalcin et al. 2011; Yilmaz et al. 2012), multivariate analysis (Komac 2006; Piegari et al. 2009; Nandi and Shakoor 2010), and logistic regression (Pradhan et al. 2008; Pradhan 2010a; Devkota et al. 2012; Choi et al. 2012; Felicisimo et al. 2012). Other different methods have been proposed by several authors, including index of entropy (Bednarik et al. 2010; Constantin et al. 2011; Pourghasemi et al. 2012c; Devkota et al. 2012; Wan 2012; Pourghasemi et al. 2012f), decision tree (Nefeslioglu et al. 2010; Yeon et al. 2012), analytical hierarchy process (Ayalew et al. 2004; Komac 2006; Yalcin 2008; Ercanoglu et al. 2008; Akgun and Turk 2010; Pourghasemi et al. 2012d; Hasekiogullari and Ercanoglu 2012), multi-criteria decision analysis (Akgun and Turk 2010; Kritikos and Davies 2011), fractal theory (Li et al. 2011), evidential belief function (Althuwaynee et al. 2012; Tien Bui et al. 2012c), and support vector machine (Yao et al. 2008; Yilmaz 2010; Marjanović et al. 2011; Xu et al. 2012; Tien Bui et al. 2012b; Ballabio and Sterlacchini 2012; Pourghasemi et al. 2012g; Pradhan 2012).

In the recent years, soft computing techniques such as artificial neural networks by (Gomez and Kavzoglu 2005; Ermini et al. 2005; Lee et al. 2007; Melchiorre et al. 2008; Nefeslioglu et al. 2008; Pradhan and Pirasteh 2010; Song et al. 2012b; Pradhan 2011c; Zare et al. 2012), fuzzy approaches (Juang et al. 1992; Binaghi et al. 1998; Ercanoglu and Gokceoglu 2002, 2004; Champati ray et al. 2007; Gorsevski and Jankowski 2008; Pourghasemi 2008; Tangestani 2009; Pradhan 2010b, c; Pradhan, 2011a, b; Pradhan et al. 2009; Akgun et al. 2012; Pourghasemi et al. 2012d), and some hybrid methods, including the neuro-fuzzy model (Kanungo et al. 2006; Lee et al. 2009; Vahidnia et al. 2010; Pradhan et al. 2010a, b; Oh and Pradhan 2011; Sezer et al. 2011; Tien Bui et al. 2011; Song et al. 2012b), and fuzzy logic analytical hierarchical process (AHP) analysis (Gorsevski et al. 2006) have been extensively used for the landslide susceptibility assessment.

The geotechnical and the safety factor model enable spatialization of landslide hazard analysis, and scenarios can be examined by changing the input parameters (Gokceoglu et al. 2000; Okimura and Kawatani 1987; Dietrich et al. 1995; Terlien et al. 1995). The main limitation of geotechnical and safety factor-based methods is that they are feasible only for areas where landslide types are simple and geomorphic and geologic properties are fairly homogeneous (Van Westen and Terlien 1996). Also, the conventional geotechnical approaches are difficult to be applied in regional landslide susceptibility assessments. The scale must be too large, and it is impossible to apply on the large areas. For this reason, we considered statistical-based approaches in the study area.

So, this paper evaluates the landslide susceptibility mapping in Tehran metropolitan using a probabilistic likelihood ratio and spatial multi-criteria evaluation models, GIS and remote sensing techniques. The main difference between the present study and the approaches described in the aforementioned publications is that a probabilistic likelihood ratio (PLR) and spatial multi-criteria evaluation (SMCE) GIS-based models were applied, and their results were compared.

## Study area

The study area is located in the north part of Tehran metropolitan, Iran between longitudes  $51^{\circ} 05' 26''$  E and  $51^{\circ} 50' 30''$  E, and latitudes  $35^{\circ} 45' 50''$  N and  $35^{\circ} 59' 16''$  N (Fig. 1). It covers an area of about  $900 \text{ km}^2$ . The altitude of the area ranges from 1,349.5 to 3,952.9 a.m.s.l. The major land use of the study area consists of rangeland and covers almost 90.5 % of it. The slope angles of the area range from  $0^{\circ}$  to as much as  $83^{\circ}$ .

The mean annual rainfall according to Fasham station in a period of 37 years is around 700 mm. Also, based on the records from the Iranian Meteorological Department (I.R. of Iran Meteorological Org (IRIMO) 2011), the maximum and minimum rainfall occurs in April and September, respectively.

According to geological survey of Iran (GSI 1997), the lithology of the study area is various, and 33.97 % of it is covered by group 5 (Table 1) such as alternation of shale and tuffaceous siltstone ( $E^{ss_3}$ ), green crystal, lithic and ash tuff, tuff breccia, and partly with intercalations of limestone ( $E^l_2$ ), alternation of shale and tuffaceous siltstone ( $E^{ts_2}$ ), rhyolitic tuff with some intercalations of shale ( $E^r_2$ ), massive green tuff, shale with dacitic and andesitic-basaltic lava flows ( $E^{tsv_1}$ ), dark grey shale with alternation of green tuff, and partly with sandstone, shale, conglomerate and limestone ( $E^{sh_1}$ ), alternation of green tuff and shale ( $E^{tsh_1}$ ), andesitic-basaltic lava breccia and lava flows ( $E^b_1$ ), rhyolitic tuff and lava flows ( $E^r_1$ ), dacitic to andesitic lava flows and rhyodacitic pyroclastic ( $E^{da_1}$ ), bituminous siltstone and shale, calcareous tuffite ( $E^{ss_1}$ ), tuffaceous sandstone, green tuff ( $E^{st_1}$ ),

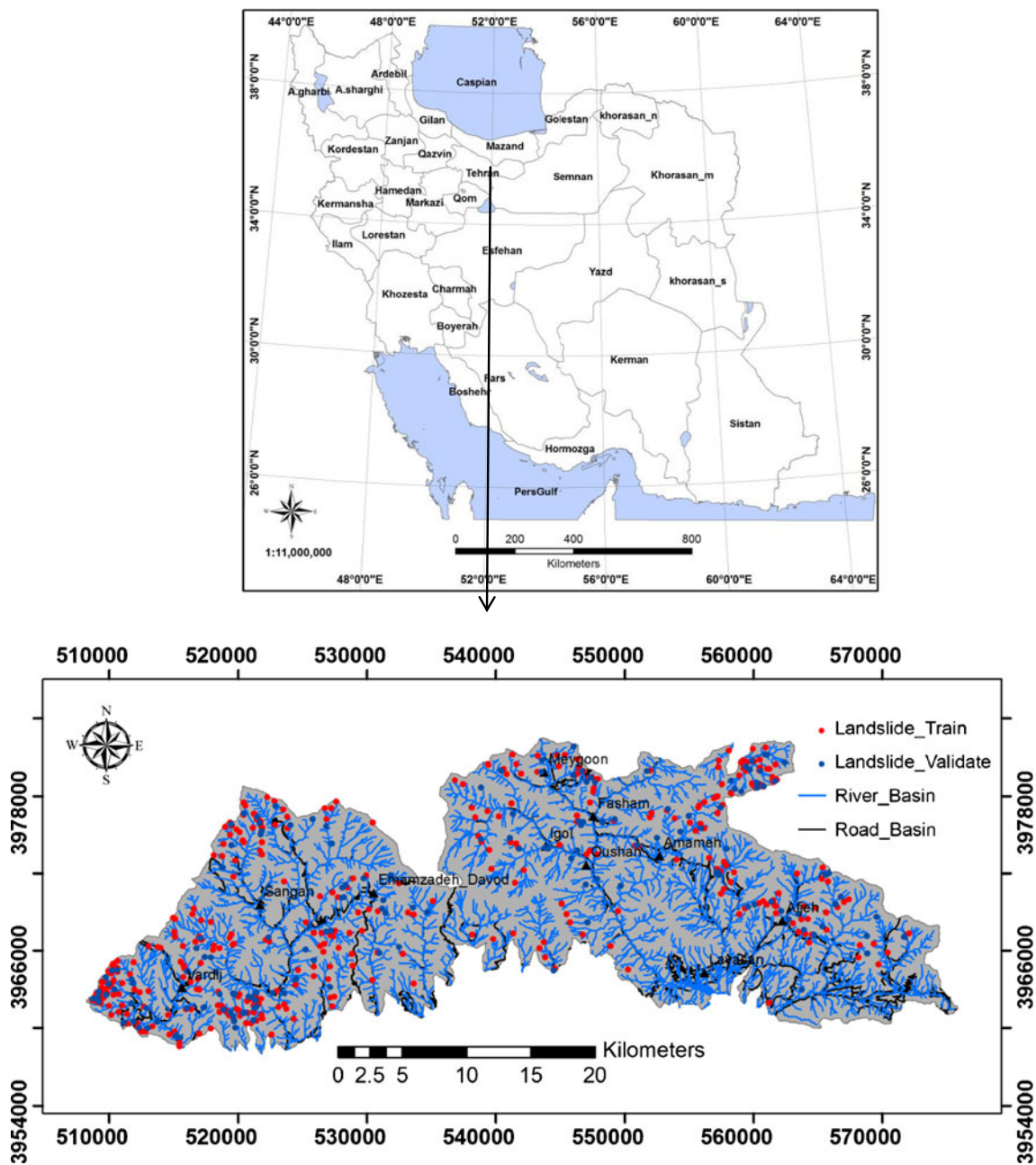


Fig. 1 Landslide location map of the study area

shales and siltstone ( $E^{sl}_1$ ), and green tuffs and limestone ( $E^{tl}_1$ ). Meanwhile 27.54 % of lithology of the study area was included by group 4 (Table 1) (GSI 1997). The most important trusts and faults of the study area include Mosha Fasham, Purkan-Vardij, north of Tehran trusts, Shirpala, and Emamzadeh Davud faults (GSI 1997).

Landslides are a very common phenomenon in the north of Tehran due to its climate condition. Most of these landslides occur near the rivers and valleys. Velenjak region located in the northwest of Tehran is one of most sensitive areas. Some other prone regions include Ozgol, Dar Abad, north of Saadat Abad, north of Emam Zadeh Ghasem, Oushan-Fasham road,

Meygoon, north of Lavasan, north of Kan, and Golab Darreh. Population density and high price of lands of these areas are the main reasons for landslide susceptibility mapping, which can be used for optimum management and also avoidance of susceptible regions.

### Spatial database

For the landslide susceptibility mapping, the main steps were data collection and construction of a spatial database from which the relevant landslide conditioning factors are extracted.

**Table 1** Lithology of the study area (GSI 1997)

Code	Group	Formation	Lithology	Geological age
Q <sup>2</sup>	1	Subrecent Tehran alluvium–unit C	Young alluvia fans and terraces	Quaternary
Q <sup>l</sup>		Kahrizak–unit B	Old alluvial fans and terraces	Quaternary
Q <sup>s</sup>		–	Young and old scree, talus deposits	Quaternary
Q <sup>f</sup>		–	Young and old alluvial fans, agglomerate	Quaternary
Q <sub>U</sub>		–	Undifferentiated young and old alluvial fans and terraces, alluvium, residual soils	Quaternary
Q <sup>al</sup>		–	Loose alluvium (including recent alluvium-unite D)	Quaternary
Q		–	Conglomeratic terraces and fans	Quaternary
Q <sup>m</sup>		–	Morain	Quaternary
Q <sup>sc</sup>		–	Scree	Quaternary
Q <sub>2</sub> <sup>t</sup>		–	Young Terraces	Quaternary
Q <sub>1</sub> <sup>t</sup>		–	Old Terraces	Quaternary
Q <sup>tr</sup>	2	–	Spongy porous travertine	Quaternary
PIQ <sup>s<sub>c</sub></sup>	3	Hezardarreh–unit A	Conglomerate, sandstone, mudstone intercalations	Pleistocene
M		Upper red	Undivided Miocene deposits including sandy marl, siltstone, conglomerate, gypsum, Miliolidus limestone	Miocene
M <sub>u</sub> <sup>2</sup>		Upper red	Sandstone, silty marl, mudstone, siltstone	Miocene
E <sub>Kn</sub>		Kond	Sandstone, conglomerate, gypsum, Nummuliti marly limestone	Eocene
E <sub>4</sub> <sup>sc</sup>		–	Sandstone, conglomerate, green tuff	Eocene
E <sub>4</sub> <sup>st</sup>		Turbiditic sediments	Light colour sandstone, greenish tuffite, conglomerate	Eocene
E <sub>3</sub> <sup>sc</sup>		–	Tuffaceous sandstone, micro-conglomerate with intercalations of tuffite	Eocene
E <sub>3</sub> <sup>tc</sup>		Turbiditic sediments	Tuffite sandstone, conglomerate	Eocene
E <sub>3</sub> <sup>sh</sup>		–	Shale with intercalations of tuffaceous sandstone and siltstone	Eocene
E <sub>f</sub> <sup>sl</sup>		–	Red conglomerate and sandstone with intercalations of limestone	Eocene
E <sub>f</sub> <sup>c</sup>		–	Red conglomerate, sandstone and shale	Eocene
E <sub>f</sub> <sup>st</sup>		–	Shale, sandstone and tuffite with intercalations of limestone	Eocene
E <sub>m</sub>		Mila	Medium-thin bedded limestone with intercalations of shales	Eocene
E <sub>z</sub>		Zagun	Red, green micaceous shales and sandstones	Eocene
PE <sub>z</sub>		Ziarat	Alveolina-Nummuliti limestone, conglomerate, gypsum	Paleocene
E <sub>K</sub> <sup>m</sup>	4	Karaj	Light green-grey laminated calcareous mudstone, shale, tuff, gypsum, tuffite	Eocene
E <sub>K</sub> <sup>t</sup>		Karaj	Green thick-bedded tuff, tuffaceous shale, minor lava, pyroclastic, tuff, breccia (mainly consisting mid. Tuff member)	Eocene
E <sub>K</sub> <sup>sh</sup>		Karaj	calcareous and siliceous dark colour shale, tuffite, pyroclastic	Eocene
E <sup>dg</sup>		–	Micro-dioritic-micro-gabbro as sill and dikes	Post Lower Eocene
E <sub>5</sub> <sup>sh</sup>		–	Shale with intercalations of tuffite and tuffaceous sandstone	Eocene
E <sub>5</sub> <sup>tb</sup>		–	Green tuff, tuff breccia, tuffite with intercalations of tuffaceous siltstone	Eocene
E <sub>5</sub> <sup>td</sup>		–	Hyalotrachyandesite, trachte-dacite, tuff breccia	Eocene
E <sub>3</sub> <sup>b</sup>	5	–	White-green tuff breccia, ash tuff	
E <sub>3</sub> <sup>ss</sup>		–	Alternation of shale and tuffaceous siltstone	Eocene
E <sub>2</sub> <sup>t</sup>		–	Green crystal, lithic and ash tuff, tuff breccia, and partly with intercalations of limestone	Eocene
E <sub>2</sub> <sup>ts</sup>		–	Alternation of shale and tuffaceous siltstone	Eocene
E <sub>2</sub> <sup>r</sup>		–	Rhyolitic tuff with some intercalations of shale	Eocene
E <sub>1</sub> <sup>tsv</sup>		–	Massive green tuff, shale with dacitic and andesitic-basaltic lava flows	Eocene
E <sub>1</sub> <sup>sht</sup>		–	Dark grey shale with alternation of green tuff, and partly with sandstone, shale, conglomerate and limestone	Eocene
E <sub>1</sub> <sup>tsh</sup>		–	Alternation of green tuff and shale	Eocene
E <sub>1</sub> <sup>b</sup>		–	Andesitic-basaltic lava breccia and lava flows	Eocene

**Table 1** (continued)

Code	Group	Formation	Lithology	Geological age
E <sub>1</sub> <sup>r</sup>		–	Rhyolitic tuff and lava flows	Eocene
E <sub>1</sub> <sup>da</sup>		–	Dacitic to andesitic lava flows and rhyodacitic pyroclastic	Eocene
E <sub>1</sub> <sup>ss</sup>		–	Bituminous siltstone and shale, calcareous tuffite	Eocene
E <sub>1</sub> <sup>st</sup>		–	Tuffaceous sandstone, green tuff	Eocene
E <sub>1</sub> <sup>sl</sup>		–	Shales and siltstone	Eocene
E <sub>1</sub> <sup>tl</sup>		–	Green tuffs and limestone	Eocene
Gy	6	–	Gypsum	Paleocene
PE <sub>f</sub> <sup>m, s, c</sup>		Fajan	Marl, sandstone, conglomerate, gypsum	Paleocene
PE <sub>f</sub> <sup>c</sup>		Fajan	Thick-bedded to massive polygenetic conglomerate, sandstone, locally limestone beds	Paleocene
PE <sup>v</sup>		–	Andesitic-dacitic rocks, red-purple agglomerate, pyroclastic, tuffs	Paleocene
K <sub>u</sub> <sup>b</sup>	7	–	Thin-bedded limestone	Turonian- Early Senonian
J <sub>1</sub>		Lar	Thin-bedded to massive limestone, in some plates may include undivided Dalihai formation	Jurassic
J <sub>d</sub>		Dalihai	Thin-bedded marly limestone, marl, Ammonite bearing	Jurassic
TR <sub>3</sub> J <sub>s</sub>		Shemshak	Shale, sandstone, siltstone, clay stone, locally limestone intercalations, coal bearing	Triassic
TR <sub>e</sub> <sup>d</sup>		Elika	Thick bedded-massive dolomites and dolomitic limestone	Triassic
TR <sub>e</sub> <sup>l</sup>		Elika	Thick-bedded to massive limestone	Triassic
TR <sub>e</sub> <sup>m, l</sup>		Elika	Platy marly limestone, Oolitic limestone	Triassic
P <sub>n</sub>		Nesen	Marly limestone	Triassic
P <sub>r</sub>		Ruteh	Medium-bedded limestone	Permian
C		Mobarak limestone	Dark grey medium bedded limestone with intercalations of marly limestone	Carbonifer
C <sub>j</sub> <sup>c</sup>		Jeirud	Light grey massive dolomitic limestone	Carbonifer
C <sub>j</sub> <sup>b</sup>		Jeirud	Black limestone, clayey marl intercalations	Carbonifer
C <sub>j</sub> <sup>d</sup>		Jeirud	Black Oolitic and intraclastic limestone	Carbonifer
m		Mobarak	Blak Oolitic, dolomitic limestone, marl intercalations	Miocene
D <sub>j</sub> <sup>a</sup>		Jeirud	Sandstone, shale, limestone, marl, phosphatic layers	Devonian
E <sub>m</sub>		Mila	Trilobite bearing limestone, marl, dolomite and shale	Eocene
E <sup>q</sup>	8	–	White quartzite, quartzitic sandstone (formly top quartzite)	Eocene
E <sub>l</sub>		Lalun	Red arkosi sandstone	Eocene
E <sub>bt</sub>		Barut	Miaeous variegated siltstone and shale, cherty dolomite intercalations	Eocene
E <sub>bt</sub> <sup>d</sup>		Barut	Black massive dolomite, green-black shale intercalations	Eocene
T <sup>b</sup>		–	Basic and intermediate sills	Tertiary, mostly Oligocene
T <sup>s</sup>		–	Mostly syenite and some leuosyenite porphyry	Tertiary, mostly Oligocene
E <sup>d</sup>		–	Dacitic dikes	lower Eocene
E <sub>6</sub> <sup>s</sup>		–	Grey-brown shale, siltstone and sandstone	Eocene

This stage is the most important part of landslide susceptibility and hazard mitigation studies (Guzzetti et al. 1999; Ercanoglu and Gokceoglu 2004; Kincal et al. 2009). The spatial database for the study area is shown in Table 2. Since landslide occurrences in the past and present are keys to future spatial prediction (Guzzetti et al. 1999), a landslide inventory map is a prerequisite for such a study. Accurate detection of landslide

locations is very important for probabilistic landslide susceptibility and hazard analysis (Pradhan and Lee 2007). In the first step, landslides were detected in the study area by interpretation of aerial photographs, satellite images, and extensive field surveys. A total of 528 landslide locations were identified and mapped in GIS at 1:25,000 scale (Fig. 1). In this research, we used the landslide classification system proposed by Varnes



**Table 2** Data used in the landslide susceptibility analysis

Scale	Source of data	Data format	Data layers
1:25,000	Satellite image, aerial photos, and field surveys	Point	Landslide inventory map
1:25,000	National Cartographic Center (NCC)	Line and point	Topographic map
1:100,000	Geology Survey of Iran (GSI)	Polygon	Geological map
LISS-III (23.5×23.5 m) and Pan (2.5×2.5 m)	National Geographic Organization (NGO)	Polygon	Land use
LISS-III (23.5×23.5 m) and Pan (2.5×2.5 m)	National Geographic Organization (NGO)	Grid	Normalized difference vegetation index (NDVI)

(1978). Most of the landslides are shallow rotational. Of 528 landslide locations, 70 % were used in landslide susceptibility mapping, and the remaining 30 % were used for validation. The size of the smallest landslide is about 685 m<sup>2</sup>. The largest landslide covers an area of 280,804 m<sup>2</sup>.

The basic data sets that have been used to generate thematic layers are the topographic maps at 1:25,000 scale, geological maps (1:100,000 scale), and the satellite IRS-P5 (LISS-III by 23.5 m spatial resolution), and the IRS-P6 (panchromatic by 2.5 m spatial resolution) remote sensing images. All the data layers were constructed on a 10×10-m grid cell, with area of 2,452 lines and 6,768 columns. A total of 17 landslide conditioning factors were taken into computations, which are slope degree, slope aspect, altitude, plan curvature, profile curvature, surface area ratio (SAR), topographic position index (TPI), topographic wetness index (TWI), slope length (LS), and sediment transport index, lithology, land use, normalized difference vegetation index (NDVI), distance from rivers, distance from roads, distance from faults, and drainage density. The contour lines for the study area were produced from 13 adjacent topographical sheets (1:25,000 scale), with the contour interval of 10 m from the national cartographic center of Iran. A digital elevation model (DEM) was created of these contour lines and points with 10-m resolution. Using this DEM, slope degree, slope aspect, altitude, plan curvature, profile curvature, SAR, and TPI were produced (Fig. 2a–g).

The slope degree is one of the most important factors that influence slope stability (Lee and Min 2001). Because the slope degree is directly related to the landslides, it was used in preparing a landslide susceptibility map. This map is prepared from the DEM, and reclassified into five categories namely: (1) 0–5°, (2) 6–15°, (3) 16–30°, 31°–50°, and (4) >50° (Fig. 2a). Slope aspect strongly affects hydrologic processes via evapotranspiration and thus affects weathering processes and vegetation and root development, especially in drier environments (Sidle and Ochiai 2006). Hence, it could be an important condition factor on landslide in the study area. Aspects are grouped into nine classes including eight directions and flat (Fig. 2b). Altitude was taken directly from a 10-m DEM and classified to six categories such as <1,500, 1,500–2,000, 2,000–2,500, 2,500–3,000, 3,000–3,500, and >3,500 m

(Fig. 2c). Altitude is an important factor on landslide occurrence because weather and climate conditions vary greatly at different elevations, and this caused differences in soil and vegetation (Aniya 1985). High altitudes may facilitate increased weathering of rocks due to freeze–thaw processes, while low elevations tend to enable thicker colluviums deposits to be formed (Dai and Lee 2001).

Plan curvature and profile curvature describe the type of slopes, and are significant factors that may cause landslides (Atkinson and Massari 2011; He et al. 2012). Plan curvature is described as the curvature of a contour line formed by intersecting a horizontal plane with the surface (Fig. 2d). The influence of plan curvature on the slope erosion processes is the convergence or divergence of water during downhill flow (Ercanoglu and Gokceoglu 2002; Oh and Pradhan 2011). The profile curvature is curvature of corresponding normal section, which is tangential to a flow line (Fig. 2e). It is negative when the normal section concavity is directed up, and positive in the opposite case (Hengl et al. 2003). It shows the flow acceleration, erosion (negative values)/deposition (positive values) rate and gives a basic idea of geomorphology (Yesilnacar 2005). In addition, the profile curvature is important because it controls the change of velocity of mass flowing down the slope (Talebi et al. 2007). The plan and profile curvature maps were produced using a system for automated geoscientific analyses GIS.

Surface area ratio is a basis for a measure of landscape topographic roughness and convolutedness (Fig. 2f). The surface area ratio of any particular region on the landscape can be calculated by the following equation (Jenness 2002):

$$SAR = \left( \frac{A}{A_s} \right) \quad (1)$$

Where  $A$  is the surface area of that region and  $A_s$  is the planimetric area. High roughness slopes are more prone to landsliding because gradient changes favor rainfall infiltration into the soil and thus its instability.

The TPI is another factor which reflects the difference in elevation between a focal cell and all cells in the neighborhood (Jenness 2002). This factor provides a simple and powerful means to classify the landscape into morphological classes

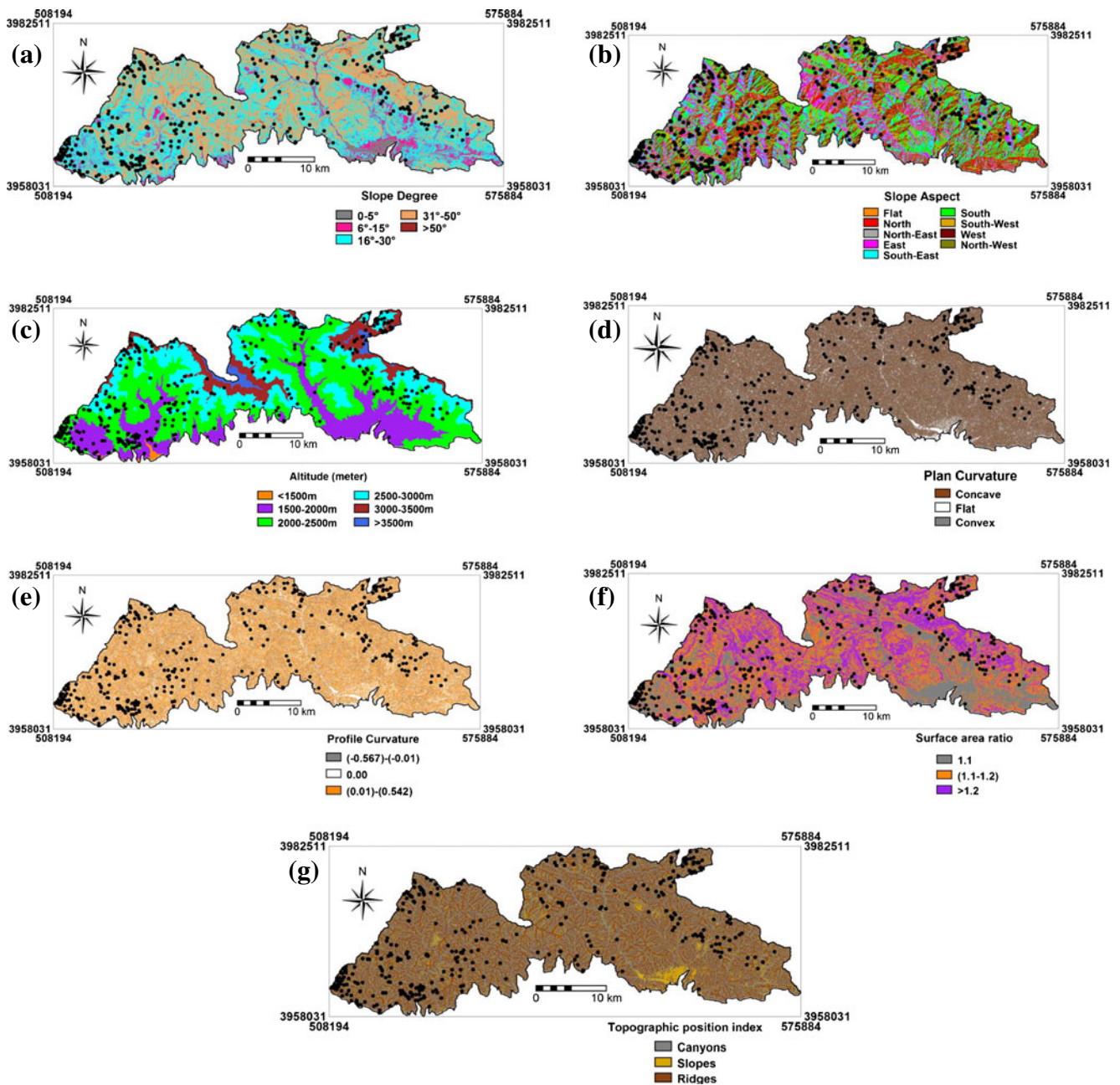


**Fig. 2** Topographical parameter maps of the study area: **a** slope degree, **b** slope aspect, **c** altitude, **d** plan curvature, **e** profile curvature, **f** surface area ratio (SAR); **g** topographic position index

(Jenness 2002). Positive and negative values indicate that the cell is higher and lower than its neighbors, respectively (Tagil and Jenness 2008; Fig. 2g).

In many publications (Yesilnacar and Topal 2005; Nefeslioglu et al. 2008; Yilmaz 2009a, b; Akgun and Turk 2010; Oh and Lee 2011; Pradhan 2011a; Pradhan et al. 2011; Wang et al. 2011; Costanzo et al. 2012; Pourghasemi et al. 2012a, b, c, d), TWI, stream power index (SPI), and LS were considered as a secondary topographical attributes for landslide susceptibility mapping (Fig. 3a–c). In the current research, these factors were computed based on the following

equations (Beven and Kirkby 1979; Moore and Burch 1986; Moore et al. 1991):

$$TWI = \left( \frac{\text{catchment area}}{\tan \beta} \right) \quad (2)$$

$$SPI = \text{catchment area} \times \tan \beta \quad (3)$$

$$\text{Slope length} = (A_s/22.13)^{0.6} \times (\sin \beta/0.0896)^{1.3} \quad (4)$$

where  $\beta$  is slope in degree.



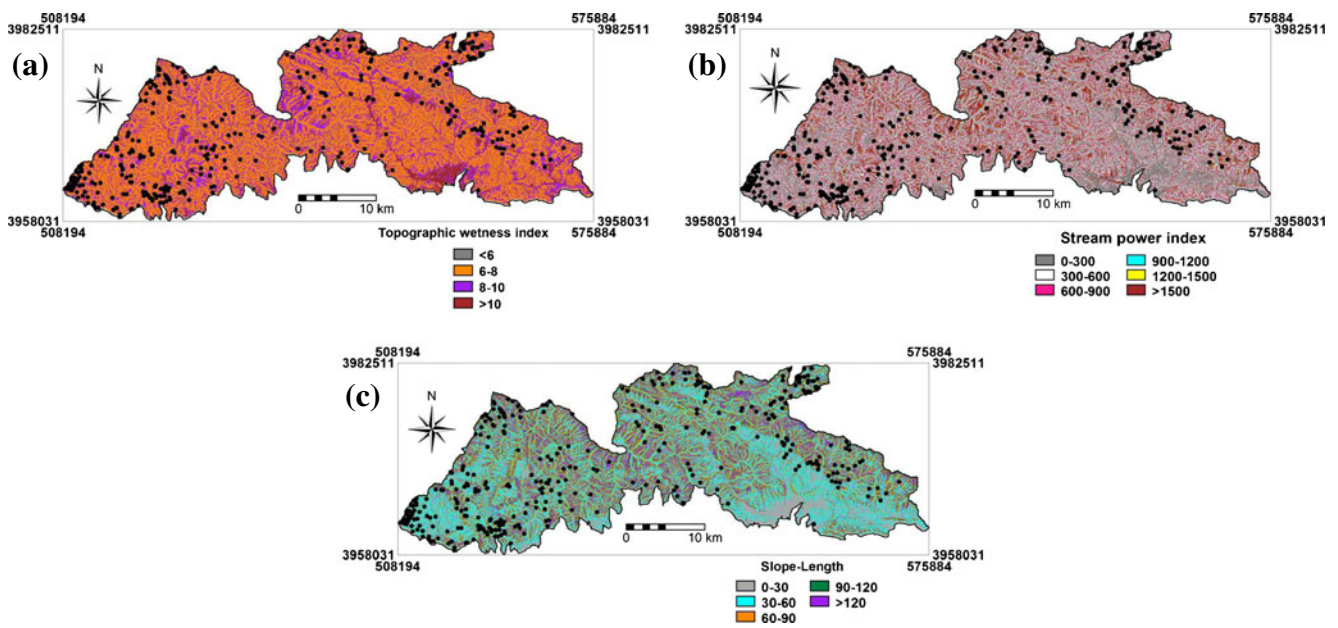


**Fig. 3** Secondary topographical attributes maps of the study area. **a** Topographic wetness index, **b** stream power index, **c** slope length

Types of lithology and structural geology play an important role in landslide susceptibility occurrence. With the impact of rainfall or an earthquake, different lithological units show substantial differences in landslide susceptibility (Song et al. 2012a). The geological maps of the study area, 1:100,000 series, sheet numbers 6,361 (east of Tehran), and 6,261 (Tehran) prepared by Geological Survey of Iran, is digitized in ILWIS 3.3 software. The study area is covered with various types of lithological units. The general geological setting of the area is shown in Fig. 4, and the lithological properties are summarized in Table 1 in detail.

The land use and NDV were derived from Indian remote sensing (IRS) images by sensors LISS III (23.5×23.5 m) and panchromatic (2.5×2.5 m). The supervised classification and maximum likelihood algorithm are assigned in order to create these maps for the study area. The land use map has been classified into eight classes such as range land, agriculture, forest, orchard, cliffs, settlement area, shrub, and water body (Fig. 5). The range land covers

almost 90.5 % of the study area. The normalized difference vegetation index (NDVI) value was calculated using the following equation:

$$\text{NDVI} = \frac{(\text{IR}-\text{R})}{(\text{IR}+\text{R})} \quad (5)$$

where IR and R values are the infrared and red portion of the electromagnetic spectrum, respectively. The NDVI (Fig. 6) is closely related to the vegetation cover. The effect of vegetation on the LSI is complex, and it is determined by the interaction of four different factors: mechanical stabilization due to the presence of roots, soil moisture depletion as a result of transpiration, surcharge from the weight of trees, and wind-breaking (Nilaweera and Nutalaya 1999; Song et al. 2012a). Overall, the large area of forest cover has a relatively low probability of landslides. Geological faults have been considered as a factor that may influence landslides. In addition, the degree of fracturing and shearing plays an important role in determining slope instability (Varnes 1984).

**Fig. 4** The lithology map of the study area

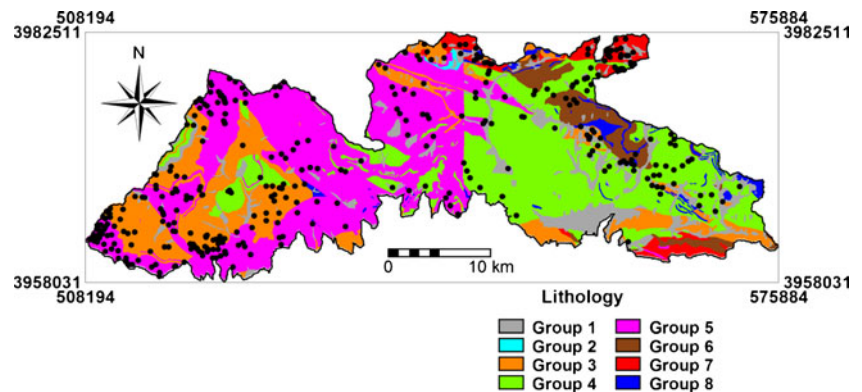
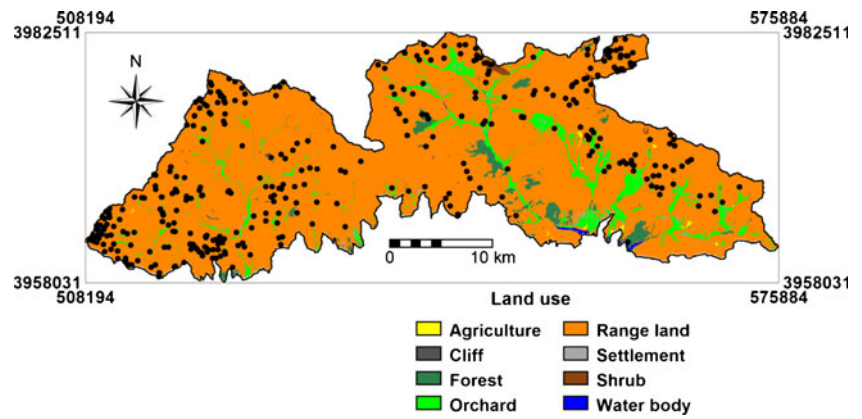


**Fig. 5** The land use map of the study area



The distance from faults map was extracted of geology maps at 1:100,000 scale, and then, buffer categories were defined as 0–200, 200–400, 400–600, 600–800, and >800 m (Fig. 7a). Distance from rivers was computed based on river networks from topographic maps. Six different buffer zones were created within the study area to determine the degree to which the streams and rivers affected the slopes (Fig. 7b). Distance from roads has been considered as one of environmental factors influencing landslides because of road cuts (Ayalew and Yamagishi 2005). Five different buffer zones are created on the path of the road to determine the effect of the road on the stability of slope (Fig. 7c). The drainage density map shows the flow of water throughout the study area and defined as the ratio of sum of the drainage lengths in the cell and the area of the corresponding cell (Sarkar and Kanungo 2004). The drainage density was computed considering a 10×10-m grid cell which ranges from 0.0002 to 0.013 km/km<sup>2</sup> and is classified into three classes (Fig. 8).

**Methodology**

**Probabilistic likelihood ratio**

In nature, the processes of landslide are quite complicated. Although many main factors that influence landslide are recognized, there are many things that recent physical models cannot consider or model. For analyzing in general inter-

relationship in landslide prediction, it is necessary to assume that landslide occurrences are determined by landslide-related factors, and that future landslides will occur under the same conditions as past landslides (Lee and Talib 2005; Lee and Pradhan 2006).

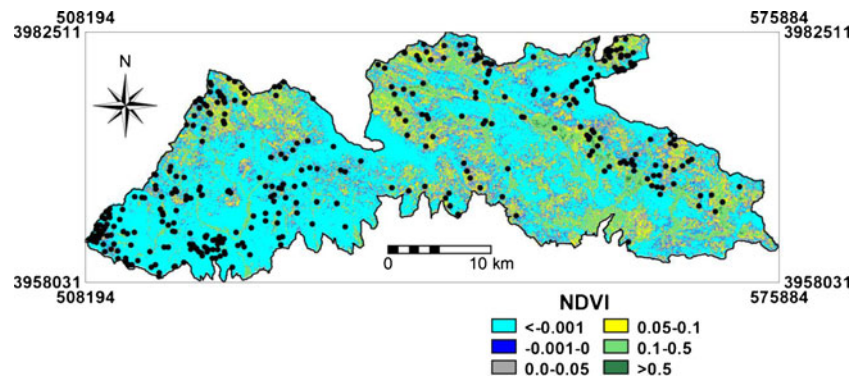
Based on this assumption, the relationships between landslides occurring in an area and the landslide-related factors can be distinguished from the relationships between landslides not occurring in an area and the landslide-related factors. The likelihood ratio represents the distinction quantitatively. It is the ratio of the area where landslides occurred to the total study area, and is the ratio of the probabilities of a landslide occurrence to a non-occurrence for a given factor’s attribute (Lee and Pradhan 2007). The probabilistic likelihood ratio (PLR) is expressed by the following equation:

$$PLR = \left( \frac{\text{no. of landslides} / \text{total of landslide}}{\text{no. of pixels in domains} / \text{total of pixels}} \right) \tag{6}$$

**Spatial multi-criteria evaluation**

Planning is a decision-making method that analyzes the problems, identifies the opportunities for changes, and appraises the alternatives taking into consideration environment, economic, and social conditions that lead to the transformation of a current situation to the best option in order to minimize costs and maximize benefits (Rahman and Saha

**Fig. 6** The NDVI map of the study area



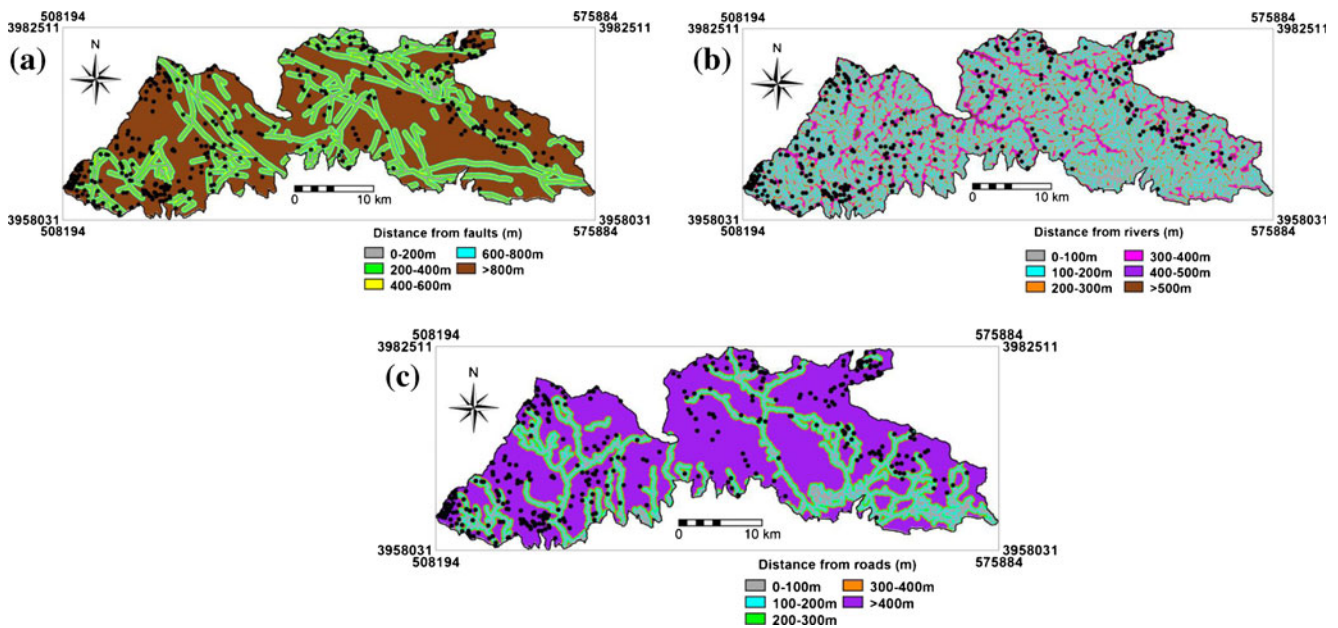


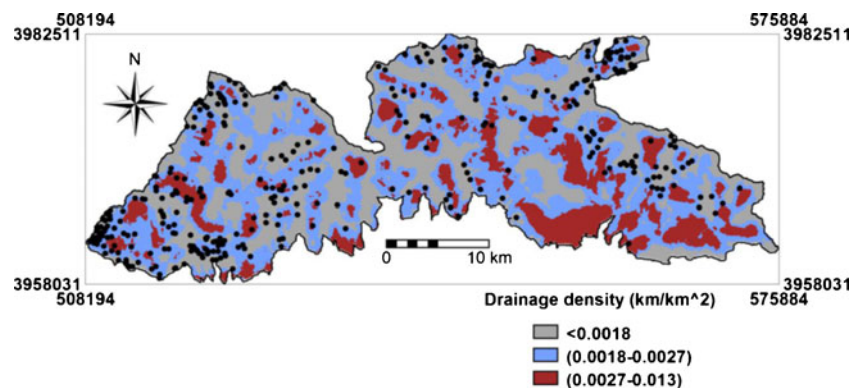
**Fig. 7** a Distance from faults, b distance from rivers, c distance from roads

2008). Landslide susceptibility mapping is a prerequisite for land use planning and hazard mitigation purpose. Due to this, we tried to use of a new technique in landslide susceptibility analysis as spatial multi-criteria evaluation. The multi-criteria evaluation (MCE) is a decision support approach in which alternatives are compared and evaluated through tree-like hierarchies of objectives and criteria (Boerboom et al. 2009). In spatial multi-criteria evaluation (SMCE), the alternatives are locations in the form of points, lines, areas, or grid cells, and therefore, criteria could occur in the form of maps (Herwijnen 1999). Thus, SMCE is an applied science-based method that combines spatial analysis using GIS and MCE to transform spatial and non-spatial input which generates output decision (Malczewski 1999; Hizbaron et al. 2011). The output of spatial multi-criteria evaluation including one or more maps of the same area as composite index maps indicates the extent to which criteria are met or not in different areas, and thereby supports planning and/or decision making (Rahman and Saha

2008). The theoretical background for the multi-criteria evaluation is based on the AHP developed by Saaty (1980). There are several phases in conducting the SMCE, such as problem tree analysis, standardization, weighting, and map generation. The problem tree analysis assumes multi-goals and multi-criteria to expose relationship among relevant criteria for main objective which generally clusters into group factors or constraints (Sharifi and Retsios 2004). Problem tree analysis covers setting up main goals, criteria, and factors. As it employs multi-criteria, thus each criterion holds certain range scale value (Hizbaron et al. 2011).

Once all the criteria and related maps or attribute tables are entered in the criteria tree, the criteria have to be standardized (Looijen 2010). The values in the various input maps have different meanings, and are probably expressed in different units of measurement (e.g., land use classes, percentages, meters, distance in meters, etc.). In order to compare the criteria with each other, all values need to be standardized, i.e., transformed to the same unit of measurement. In order to

**Fig. 8** The drainage density map of the study area





standardize input maps in SMCE environment, one of the standardization methods such as numerical, Boolean, and qualitative methods can be used (Nafoti and Chabok Boldaje 2011). An output standardization value of 0 means that the input value is perceived to have low landslide susceptibility, and an output standardization value of 1 means that the input value is perceived to have high landslide susceptibility. Finally, the landslide conditioning factors are weighted by means of direct, pairwise, and rank ordering comparison, and the output is a composite index map (Castellanos and Van Westen 2007). Figure 9 presents an overview of the various components of the landslide susceptibility method.

**Results**

**Probabilistic likelihood ratio**

The results of spatial relationship between landslide and conditioning factors using probabilistic likelihood ratio model are shown in Table 2. In the mentioned Table, for the slope degree between 16° and 30°, the PLR was 1.23, which indicates a very high probability of landslide occurrence. It can be noticed that 52.43 % of landslides occurs in this class. Similarly, for the slope degree between 0° and 5°, 6° and 15°, and >50°, the ratio was <1 (0.12, 0.27, and 0.38, respectively), which indicates a very low and low probability of landslide occurrence. In the study area, we observed

that when slope gradient is increasing, frequency ratio is decreasing. Althuwaynee et al. (2012) reported that with the slope between 0° and 15°, the value is lower because of the direct proportion between slope and failure. In the case of slope aspect, landslides were most abundant on northeast-facing (1.89), east-facing (1.32), and north-facing (1.27) slopes. Thus, slopes facing to those are highly susceptible to landslides, whereas the frequency ratio of landslide was lowest on flat and south-facing slopes. In the study area, these facings have higher humidity, so are very susceptible to landslide occurrence. The relationship between landslide occurrence and altitude reflects that the elevations between 2,000 and 2,500 m; 2,500 and 3,000 m; and 3,000 and 3,500 m have a frequency ratio >1, indicating that the probability of occurrence of landslide in these altitudes is high. Meanwhile, altitude >3,500 m has a low frequency ratio (0.61). Pachauri and Pant (1992) stated that the higher elevation shows a greater susceptibility to sliding. However, in this research and based on the results of Ercanoglu and Gokceoglu (2002), the higher topographical elevation is formed by the lithological units resistant to landslide and has a low frequency ratio. Based on the results of the probabilistic likelihood ratio model (Table 1), the more positive or negative the curvature value, the higher the probability of landslide occurrence. Flat areas had a low curvature value of 0.79, whereas convex-shaped areas had the highest value of 1.03. The reason for this is that a convex rounded hilltop slope could be exposed to repeated dilation

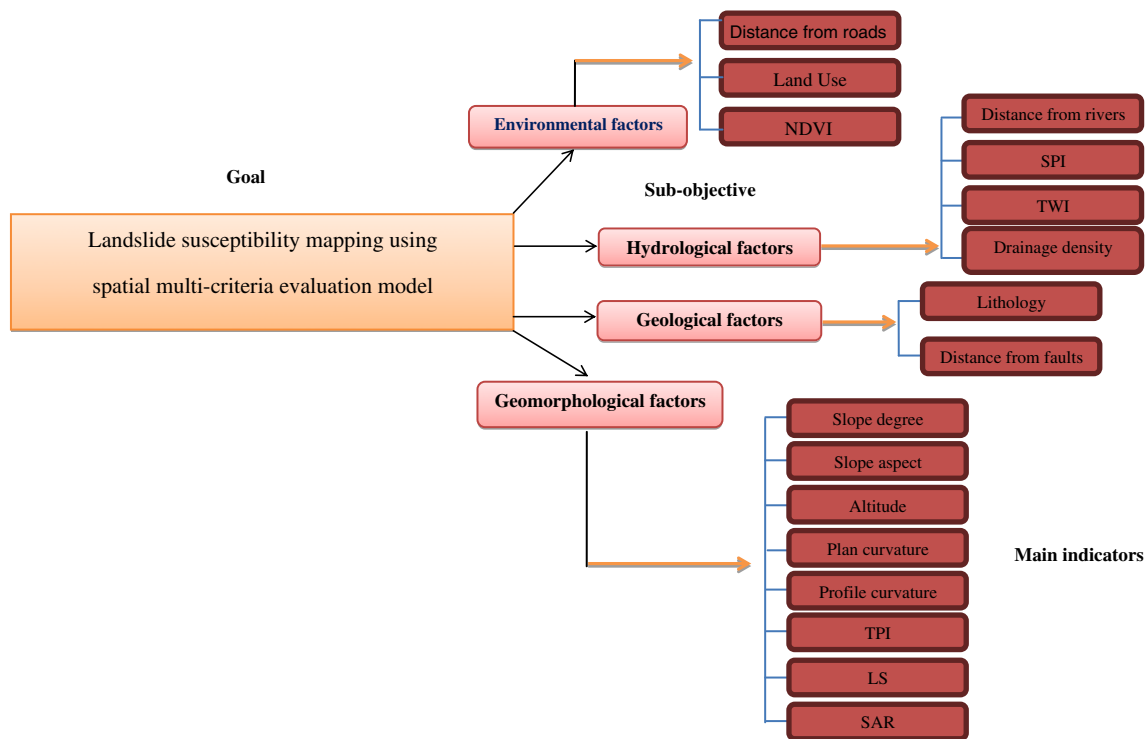


**Fig. 9** The flow chart for landslide susceptibility mapping using the SMCE model in the study area

**Table 3** Spatial relationship between landslides and landslide conditioning factors

Factor	Class	<i>A</i>	<i>B</i>	<i>C</i>	<i>D</i>	PLR (D/B)	Fuzzy value	Standardized method
Slope degree	0–5°	208,056	2.32	1	0.27	0.12	0.1	Concave
	6–15°	810,093	9.01	9	2.43	0.27	0.21	
	16–30°	3,821,708	42.51	194	52.43	1.23	0.9	
	31–50°	4,084,952	45.44	165	44.60	0.98	0.72	
	>50°	64,615	0.72	1	0.27	0.38	0.29	
Slope aspect	Flat	2,311	0.03	0	0	0	0.1	Interval
	North	746,415	8.30	39	10.54	1.27	0.64	
	Northeast	925,769	10.3	72	19.46	1.89	0.9	
	East	1,164,311	12.95	63	17.03	1.32	0.66	
	Southeast	1,261,381	14.03	43	11.62	0.83	0.45	
	South	1,410,918	15.70	39	10.54	0.67	0.38	
	Southwest	1,488,757	16.56	46	12.43	0.75	0.42	
	West	1,139,281	12.67	33	8.92	0.70	0.4	
	Northwest	850,281	9.46	35	9.46	1	0.52	
Altitude (m)	<1,500	28,167	0.31	1	0.27	0.87	0.49	Concave
	1,500–2,000	1,794,843	19.97	49	13.24	0.66	0.18	
	2,000–2,500	3,742,774	41.63	164	44.33	1.07	0.79	
	2,500–3,000	2,386,544	26.55	112	30.27	1.14	0.9	
	3,000–3,500	878,385	9.77	40	10.81	1.11	0.85	
Plan curvature (100/m)	Concave	3,730,908	41.50	154	41.62	1.00	0.8	Concave
	Flat	768,185	8.55	25	6.76	0.79	0.1	
	Convex	4,490,331	49.95	191	51.62	1.03	0.9	
Profile curvature (100/m)	(–0.567)–(–0.01)	1,408,397	15.67	45	12.16	0.78	0.1	Concave
	0	6,238,519	69.40	277	74.87	1.08	0.9	
	0.01)–(–0.542))	1,342,508	14.93	48	12.97	0.87	0.34	
Surface area ratio (SAR)	<1.10	2,743,115	30.51	83	22.43	0.74	0.1	Concave
	1.10–1.20	3,467,844	38.58	174	47.03	1.22	0.9	
	>1.20	2,778,465	30.91	113	30.54	0.99	0.52	
Topographic position index (TPI)	Canyons	3,906,746	43.46	160	43.24	0.99	0.24	Concave
	Slopes	1,066,419	11.86	54	14.6	1.23	0.9	
	Ridges	4,016,259	44.68	156	42.16	0.94	0.1	
Topographic wetness index (TWI)	<6	180,568	2.01	4	1.08	0.54	0.36	Concave
	6–8	5,297,896	58.93	228	61.62	1.05	0.74	
	8–10	2,499,080	27.80	130	35.14	1.26	0.9	
	>10	1,011,880	11.26	8	2.16	0.19	0.1	
Stream power index (SPI)	0–300	2,108,573	23.46	56	15.13	0.65	0.1	Concave
	300–600	1,984,601	22.08	97	26.22	1.19	0.64	
	600–900	1,288,914	14.34	77	20.81	1.45	0.9	
	900–1,200	799,175	8.89	36	9.73	1.09	0.54	
	1,200–1,500	512,775	5.70	24	6.49	1.14	0.59	
Slope-length (LS)	0–30	1,332,777	14.82	25	6.76	0.46	0.1	Concave
	30–60	2,789,349	31.03	134	36.22	1.17	0.86	
	60–90	2,552,783	28.40	127	34.32	1.21	0.9	
	90–120	1,147,793	12.77	49	13.24	1.04	0.72	
	>120	1,166,722	12.98	35	9.46	0.73	0.39	
Lithology	Group 1	919,687	10.23	22	5.95	0.58	0.3	Interval
	Group 2	15,945	0.18	0	0	0	0.1	
	Group 3	1,597,077	17.77	87	23.51	1.32	0.55	
	Group 4	2,474,738	27.53	66	17.84	0.65	0.32	



**Table 3** (continued)

Factor	Class	<i>A</i>	<i>B</i>	<i>C</i>	<i>D</i>	PLR ( <i>D/B</i> )	Fuzzy value	Standardized method
Land use	Group 5	3,055,530	33.99	150	40.54	1.19	0.5	Interval
	Group 6	426,844	4.75	7	1.89	0.40	0.24	
	Group 7	308,607	3.43	30	8.11	2.36	0.9	
	Group 8	190,996	2.12	8	2.16	1.02	0.45	
	Agriculture	12,673	0.14	0	0	0	0.1	
	Cliff	9,643	0.11	0	0	0	0.1	
	Forest	207,254	2.31	4	1.08	0.47	0.44	
	Orchard	540,179	6.01	1	0.27	0.04	0.13	
	Range land	8,137,410	90.51	365	98.65	1.09	0.9	
	Settlement	49,206	0.55	0	0	0	0.1	
NDVI	Shrub	17,666	0.2	0	0	0	0.1	Maximum
	Water body	15,393	0.17	0	0	0	0.1	
	<-0.001	5,104,044	56.78	234	63.24	1.11	0.89	
	-0.001-0.00	389,157	4.33	12	3.24	0.75	0.63	
	0.0-0.05	1,579,113	17.57	62	16.76	0.95	0.77	
	0.05-0.1	835,563	9.29	39	10.54	1.13	0.9	
Distance from faults (m)	0.1-0.5	1,060,265	11.79	23	6.22	0.53	0.48	Maximum
	>0.5	21,282	0.24	0	0	0	0.1	
	0-200	1,053,403	11.72	33	8.92	0.76	0.2	
	200-400	988,251	10.99	36	9.73	0.89	0.39	
	400-600	877,027	9.76	25	6.76	0.69	0.1	
	600-800	785,670	8.74	40	10.81	1.24	0.9	
Distance from rivers (m)	>8,000	5,285,073	58.79	236	63.78	1.09	0.68	Maximum
	0-100	3,587,993	39.91	116	31.35	0.79	0.45	
	100-200	2,612,101	29.06	121	32.70	1.13	0.72	
	200-300	1,623,562	18.06	91	24.60	1.36	0.9	
	300-400	819,441	9.12	30	8.11	0.89	0.53	
	400-500	276,267	3.07	11	2.97	0.97	0.59	
Distance from roads (m)	>500	70,060	0.78	1	0.27	0.35	0.1	Maximum
	0-100	1,066,777	11.87	17	4.59	0.39	0.1	
	100-200	826,979	9.20	23	6.22	0.68	0.4	
	200-300	689,664	7.67	30	8.11	1.06	0.79	
	300-400	622,091	6.92	30	8.11	1.17	0.9	
River density (km/km <sup>2</sup> )	>400	5,783,913	64.34	270	72.97	1.13	0.86	Maximum
	<0.0018	3,296,904	36.67	166	44.86	1.22	0.9	
	(0.0018-0.0027)	3,954,210	43.99	168	45.41	1.03	0.69	
	(0.0027-0.013)	1,738,310	19.34	36	9.73	0.50	0.1	

Total of landslides=370; total of pixels in domain=8,989,424

*A* number of pixels in domain, *B* percentage pixels in domain, *C* number of landslides, *D* percentage of landslides, *PLR* probabilistic likelihood ratio

and contraction of loose debris on an inclined surface that might induce a creeping or mudslide due to heavy rainfall.

In the case of profile curvature, most of the landslides occurred in straight class with *PLR* value of 1.08. This means that the landslide probability is higher in this class. In profile curvatures, slope stability slightly increases when plan shape changes from concave to convex. However, this effect is more pronounced when it changes from straight to convex. For surface area ratio factor, the value 1 represents smooth areas, and higher values represent roughness parts.

So, the frequency ratio for the SAR was high in 1.1-1.2 class, which indicates a high probability of landslide occurrence. The topographic position index value showed that slopes are considered to be susceptible to landslide process with values 1.23 than canyons and ridge areas. In the case of topographic wetness index, the higher frequency ratio values were found for classes of 8-10 (1.26) and 6-8 (1.05), whereas the *TWI* >10 has the least susceptibility probability to landslide (*PLR*=0.19). This factor describes the effect of topography on the location and size of saturated source areas of runoff generation under the

**Table 4** Scale of preference between two parameters in AHP (Saaty 1980)

Scales	Degree of preference	Explanation
1	Equally	Two activities contribute equally to the objective
3	Moderately	Experience and judgment slightly to moderately favor one activity over another.
5	Strongly	Experience and judgment strongly or essentially favor one activity over another.
7	Very strongly	An activity is strongly favored over another and its dominance is showed in practice.
9	Extremely	The evidence of favoring one activity over another is of the highest degree possible of an affirmation.
2, 4, 6, 8	Intermediate values	Used to represent compromises between the preferences in weights 1, 3, 5, 7, and 9.
Reciprocals	Opposites	Used for inverse comparison.

assumption of steady-state conditions and uniform soil properties (i.e., transmissivity is constant throughout the catchments and equal to unity). The SPI is a measure of the erosive power of water flow based on the assumption that discharge ( $q$ ) is proportional to a specific area of a catchment. Relation between stream power index and landslide occurrence probability showed classes of 600–900 and 0–300 and have values of 1.45 and 0.65, respectively. Similarly, for slope length, class 60–90 has the most frequency ratio value (1.21). Thus, this class is very susceptible and hazardous to landslide process. The slope length revealed that the physical meaning of this factor is the extent of sediment transportation controlled by a specific area of a catchment and the slope gradient. For lithology factor, groups 7 and 3 (see in details in Table 1) have a high frequency ratio (2.36, 1.32), indicating that the probability of occurrence of landslide in these lithological units is high. In case of lithology, group 2 has a value 0.00, thus is non-susceptible to landslide. In the case of land use, it can be seen that 98.65 % of landslide falls on rangeland area with value of 1.09, indicating that the probability of occurrence of landslide in this land use type is very high. The NDVI factor shows that the range between 0.05–0.1 and >0.5 is relatively favorable (high susceptible) and unfavorable (non-susceptible) for

**Table 5** The weight value of each group using pairwise comparison for the SMCE model

Inconsistency ratio=0.0398

Group factors	Environmental	Hydrological	Geological	Geomorphological	Weight
Environmental	1	–	–	–	0.180
Hydrological	1/3	1	–	–	0.088
Geological	2	3	1	–	0.272
Geomorphological	3	4	2	1	0.460

landslide occurrence. Their PLR values are 1.13 and 0.00, respectively. In the range between 0.05–0.1 and >0.5, the study area generally covers by sparse vegetation and dense vegetation and tropical rainforest, respectively. Distance 600–800 and above 800 m from faults show high favorability to landsliding compared to the other classes. The result of distance from rivers shows that class between 100–200 and 200–300 m is considered to be susceptible with values 1.13 and 1.36, respectively. The farther the distance from the rivers, the lower the landslide occurrence probability compared to areas close to the rivers.

Assessment of distance from roads showed that distances of 300–400 and >400 m have high correlation with landslide occurrence. According to the frequency ratio and its results for road buffers, landslide pixels proportionally increase with increased distance from roads. While this appears to go against the visible pattern of more failures close to roads, it is likely due to a few large landslides where no roads are present. As a result, the large slides increase the percentage of landslide pixels occurring far from roads. The drainage density <0.0018 km/km<sup>2</sup> has the largest frequency ratio value (PLR=1.22), which means the attributes of this class have the strongest relationship with landslide occurrence. It can be observed that as the drainage density increases, the landslide frequency generally decreases. Several researches (Pachauri et al. 1998; Nagarajan et al. 2000; Cevik and Topal 2003; Yalcin 2005) emphasized that the higher drainage density, the lower infiltration and the faster movement of surface flow.

Finally, the probabilistic likelihood ratios of each factor's type or class were summed to calculate the landslide susceptibility map (LSM), as shown in Eq. 7 (Lee 2004):

$$LSM_{PLR} = \sum_{i=1}^{17} PLR \quad (7)$$

In the above equation, if the LSM value is high, it means a higher susceptibility to landslide; a lower value means a lower susceptibility to landslides (Lee 2004).

#### Spatial multi-criteria evaluation

Spatial multi-criteria evaluation is a technique that assists stakeholders in decision making with respect to a special goal. It is an ideal tool for transparent group decision making, using spatial criteria, which are combined and weighted with respect to the overall goal (Van Westen 2012). After the selection of the indicators, their standardization, and the

definition of indicator weights, the analysis was carried out using an ILWIS GIS script to obtain the composite index maps and the final landslide susceptibility map.

The SMCE was built based on analyzing the weight value in bivariate statistical analysis for classes of conditioning factors (Table 3). In the next step, weight value of these factors is standardized from their original values to the value range of 0–1. It is important to notice that the indicators have different measurement scales (nominal, ordinal, and interval). The standardization process is different if the indicator is a “value” map with numerical and measurable values (interval and ratio scales) or a “class” map with categories or classes (nominal and ordinal scales). For standardizing value maps, a set of equations can be used to convert the actual map values to a range between 0 and 1 (Nafooti and Chabok Boldaje 2011). In this research, for standardization of the scale in thematic layers the fuzzy logic method was used. The fuzzy set representations of the conditioning parameters of the landslides are obtained as follows:

1.  $\mu_S$  Slope degree=(0.1/1, 0.21/2, 0.9/3, 0.72/4, 0.29/5).
2.  $\mu_S$  Slope aspect=(0.1/1, 0.64/2, 0.9/3, 0.66/4, 0.45/5, 0.38/6, 0.42/7, 0.4/8, 0.52/9).
3.  $\mu_S$  Altitude=(0.49/1, 0.18/2, 0.79/3, 0.9/4, 0.85/5, 0.1/6).
4.  $\mu_S$  Plan curvature=(0.8/1, 0.1/2, 0.9/3).
5.  $\mu_S$  Profile curvature=(0.1/1, 0.9/2, 0.34/3).
6.  $\mu_S$  SAR=(0.1/1, 0.9/2, 0.52/3).
7.  $\mu_S$  TPI=(0.24/1, 0.9/2, 0.1/3).
8.  $\mu_S$  TWI=(0.36/1, 0.74/2, 0.9/3, 0.1/4).
9.  $\mu_S$  SPI=(0.1/1, 0.64/2, 0.9/3, 0.54/4, 0.59/5, 0.3/6).
10.  $\mu_S$  LS=(0.1/1, 0.86/2, 0.9/3, 0.72/4, 0.39/5).
11.  $\mu_S$  Lithology=(0.3/1, 0.1/2, 0.55/3, 0.32/4, 0.5/5, 0.24/6, 0.9/7, 0.45/8).
12.  $\mu_S$  Land use=(0.1/1, 0.1/2, 0.44/3, 0.13/4, 0.9/5, 0.1/6, 0.1/7, 0.1/8).
13.  $\mu_S$  NDVI=(0.89/1, 0.63/2, 0.77/3, 0.9/4, 0.48/5, 0.1/6).
14.  $\mu_S$  Distance from faults=(0.2/1, 0.39/2, 0.1/3, 0.9/4, 0.68/5).
15.  $\mu_S$  Distance from rivers=(0.45/1, 0.72/2, 0.9/3, 0.53/4, 0.59/5, 0.1/6).
16.  $\mu_S$  Distance from roads=(0.1/1, 0.4/2, 0.79/3, 0.9/4, 0.86/5).
17.  $\mu_S$  Drainage density=(0.9/1, 0.69/2, 0.1/3).

**Table 6** The weight value of environmental factors by analytical hierarchy process (AHP)

Environmental factors	Distance from road	Land use	NDVI	Weight
Distance from road	1	1/3	1/2	0.164
Land use	–	1	2	0.539
NDVI	–	–	1	0.297

Inconsistency ratio=0.0096

**Table 7** The weight value of hydrological factors by analytical hierarchy process (AHP)

Hydrological factors	Distance from river	SPI	TWI	Drainage density	Weight
Distance from rivers	1	3	4	2	0.477
SPI	–	1	1	1/2	0.138
TWI	–	–	1	1/2	0.128
Drainage density	–	–	–	1	0.256

Inconsistency Ratio=0.0048

All comparisons are based on pairwise method proposed by Saaty (1980) namely analytical hierarchy process (Table 4). AHP is a multi-objective, multi-criteria decision-making approach which enables the user to arrive at a scale of preference drawn from a set of alternatives (Saaty 1980). Generally, criteria for landslide susceptibility mapping are divided in four groups (sub-objectives) such as environmental, hydrological, geological, and geomorphological factors. They are the input for the SMCE analysis. Each group will be represented by several indicators:

(a) the environmental group consists of distance from road, land use, and NDVI; (b) hydrological group includes distance from river, stream power index, topographic wetness index, and drainage density; (c) geological group contains lithology and distance from faults; (d) geomorphological factors consist of slope degree, slope aspect, altitude, plan curvature, profile curvature, topographic position index, slope length, and surface area ratio (Fig. 9). Using the AHP method, the levels of the influence of sub-objectives were generated (Table 5). Based on our results in expert choice software, it can be seen that geomorphological factor has the most influence on landslide occurrence (0.460). On the other hand, the environmental factor which has less influence was categorized in the lowest level (0.088). Also, weight value of main indicators for the study area was calculated by analytical hierarchy process (Tables 6, 7, 8, and 9). Based on the results in Table 6 (environmental factors), it can be seen that land use conditioning factor is more susceptible to landslide (weight value=0.539). On the other hand, the distance from roads is less prone to landslide as it has value of 0.164. For hydrological factors (Table 7), weight corresponding to distance from rivers (0.477) is large, whereas topographic wetness index is lowest (0.128). In geological factors (Table 8), lithology has a

**Table 8** The weight value of geological factors by analytical hierarchy process (AHP)

Geological factors	Lithology	Distance from fault	Weight
Lithology	1	5	0.833
Distance from fault	–	1	0.167

Inconsistency ratio=0.00

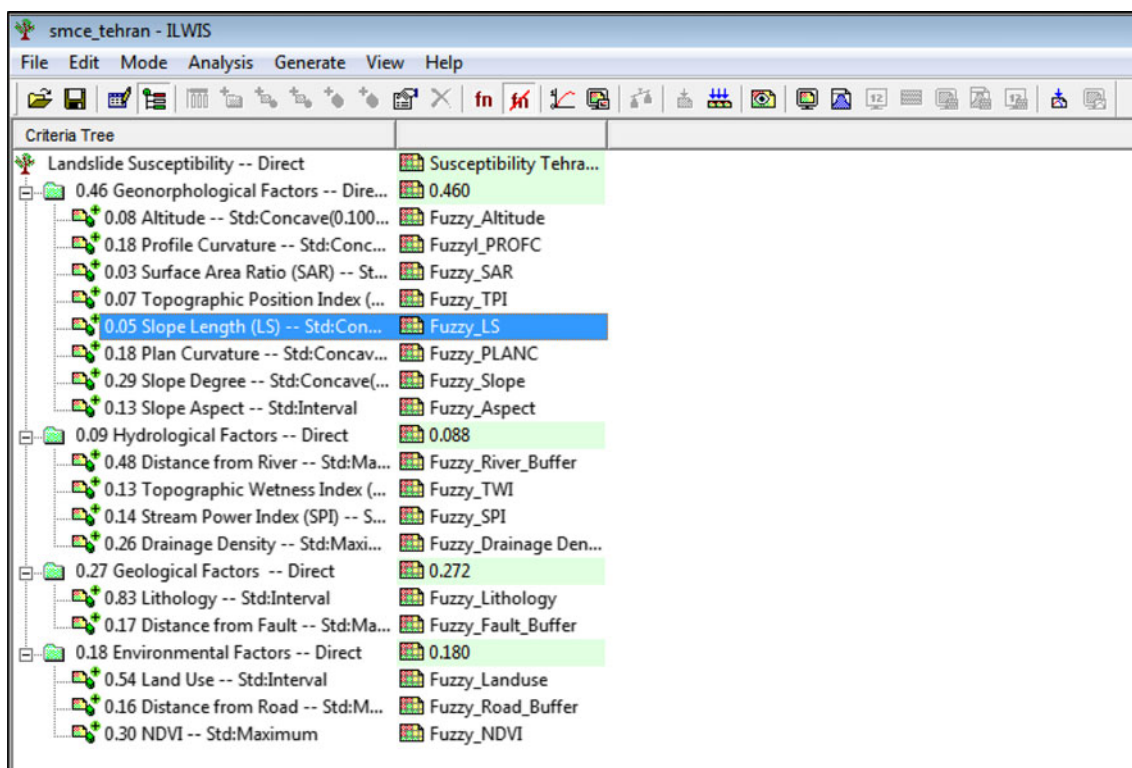
**Table 9** The weight value of geomorphological factors by analytical hierarchy process (AHP)

Geomorphological factors	Slope	Aspect	Altitude	Plan curvature	Profile curvature	TPI	LS	SAR	Weight
Slope	1	3	4	2	2	5	5	6	0.293
Aspect	–	1	2	1/2	1/2	3	3	5	0.126
Altitude	–	–	1	1/3	1/3	2	2	4	0.082
Plan curvature	–	–	–	1	1	3	3	5	0.176
Profile curvature	–	–	–	–	1	3	3	5	0.176
TPI	–	–	–	–	–	1	2	4	0.067
LS	–	–	–	–	–	–	1	3	0.053
SAR	–	–	–	–	–	–	–	1	0.028

Inconsistency ratio=0.0405

higher probability of occurrence than the distance from fault and therefore received a higher weight (0.833 vs. 0.167). In the case of geomorphological factors (Table 9), it was observed that slope degree, slope aspect, plan curvature, profile curvature, altitude, TPI, LS, and SAR have a weight value of 0.293, 0.126, 0.176, 0.176, 0.082, 0.067, 0.053, and 0.028, respectively. As a result, the slope degree is highly prone to landslide occurrence, and in contrary, surface area ratio has the lowest impact in landslide susceptibility. For all cases of the gained class weights (sub-objective and indicators), the inconsistency ratios are less than 0.1; the ratio indicates a reasonable level of consistency in the pairwise comparison that was good enough to recognize the class weights.

Finally, the spatial multi-criteria evaluation for study area was designed in tree model in SMCE module of ILWIS software (Fig. 10). Based on the criteria identified and the spatial multi-criteria evaluation performed, landslide susceptibility maps (composite index maps) for each of the four considered groups were generated. These are shown in Fig. 11. Finally, the final landslide susceptibility map by SMCE model was created by aggregation of composite index maps of sub-objectives to the overall composite index map. The landslide susceptibility maps (SMCE and PLR) were reclassified into four relative susceptibility classes: high, moderate, low, and very low (Fig. 12) based on natural break classification scheme (Pourghasemi et al. 2012c, e).

**Fig. 10** Designed criteria tree model in SMCE



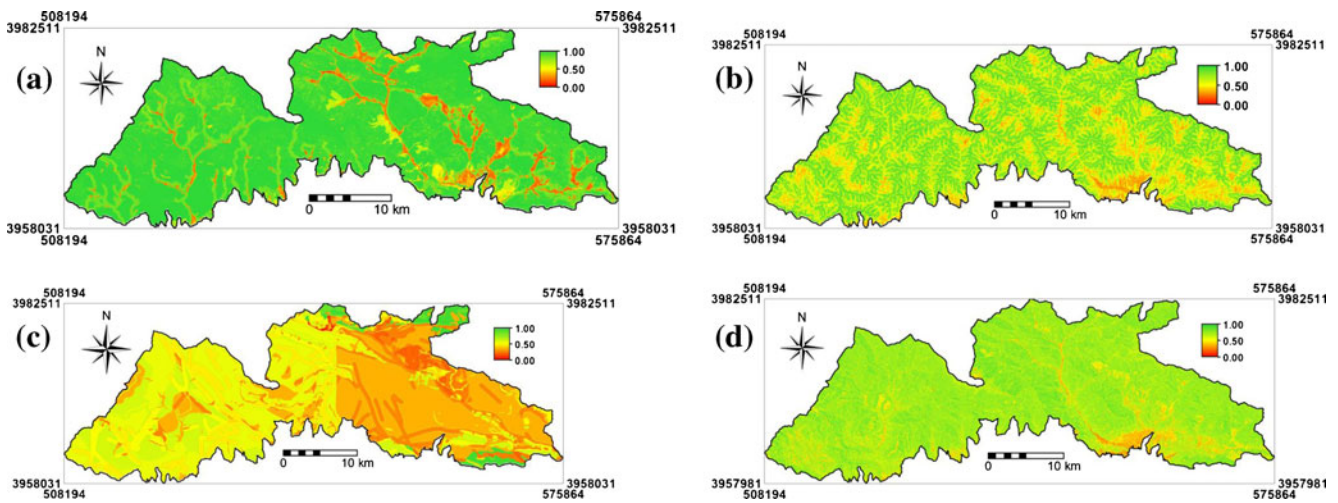


**Fig. 11** Composite index maps each of the four considered groups: **a** environmental, **b** hydrological, **c** geological, **d** geomorphological

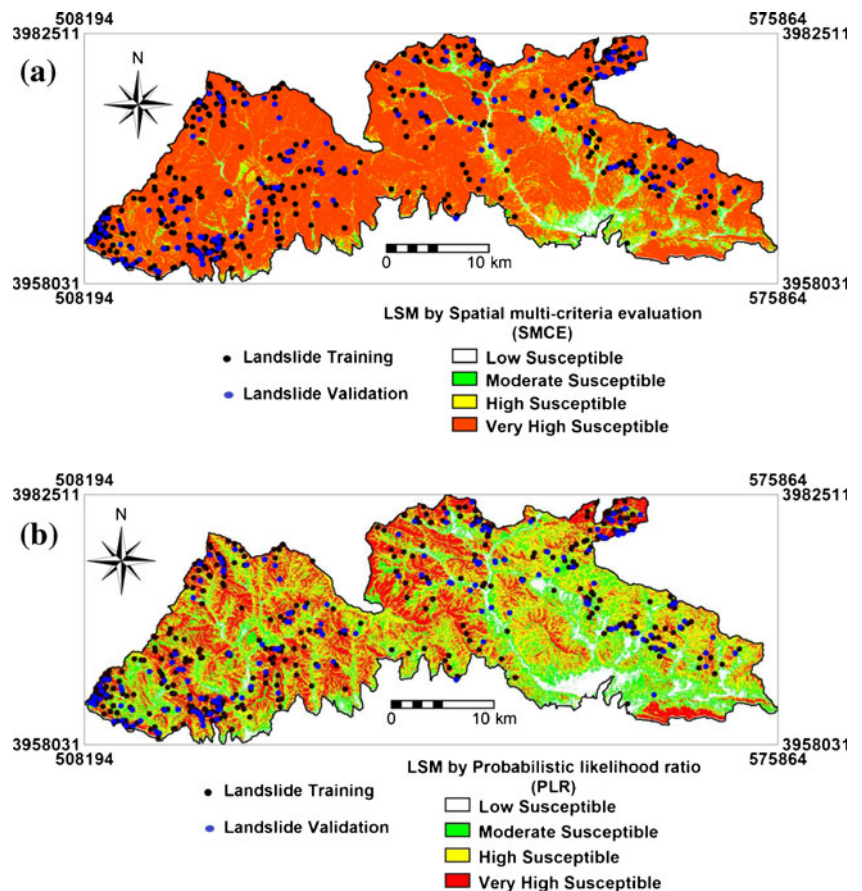
**Validation of the landslide susceptibility map**

In landslide susceptibility modeling, the most important component is to perform validation of the prediction results. Without validation, the predicted model and prepared maps are totally wasteful and have any scientific significance (Chung and Fabbri 2003). Three basic techniques can be used to obtain an independent sample of landslide for

validating a landslide susceptibility map (Remondo et al. 2003; Irigaray et al. 2007):

1. The original inventory is randomly split into two groups, one for the susceptibility analysis and one for validation;
2. The analysis is carried out in a part of the study area, and the susceptibility map thus prepared is tested in another part with different landslides;

**Fig. 12 a** Landslide susceptibility map based on spatial multi-criteria evaluation (SMCE), **b** landslide susceptibility map based on probabilistic likelihood ratio (PLR)





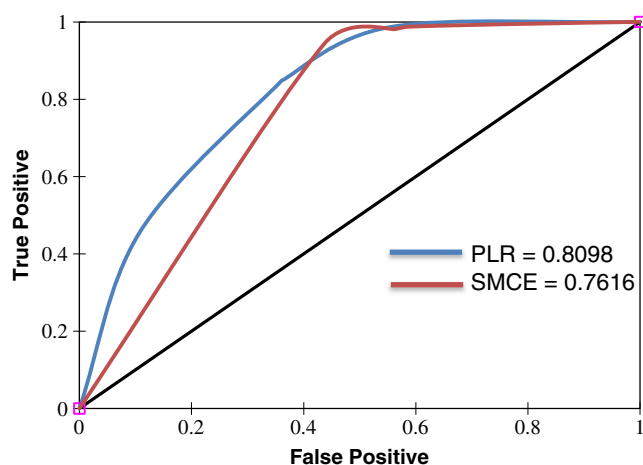


**Fig. 13** ROC curve for the susceptibility maps produced in this study

- The analysis is made using landslides generated in a certain period, and validation is performed by means of landslides that occurred in a different period. In this research, we used the first method which was proposed by several researches (Lee et al. 2009; Oh and Lee 2010; Oh and Pradhan 2011; Pradhan et al. 2011, Tien Bui et al. 2012a; Pourghasemi et al. 2012c; Devkota et al. 2012).

#### Receiver operating characteristic curves

The receiver operating characteristic (ROC) curve is a useful method of representing the quality of deterministic and probabilistic detection and forecast systems (Swets 1988). The area under the ROC curve (AUC) characterizes the quality of a forecast system by describing the system's ability to anticipate correctly the occurrence or non-occurrence of pre-defined "events" (Negnevitsky 2002). The ROC curve plots the false positive rate on the  $X$  axis and the true positive rate on the  $Y$  axis. It shows the trade-off between the two rates (Negnevitsky 2002). The ROC curves can be summarized quantitatively with the help of the area under the ROC curve, which will give the accuracy of the developed model for predicting the landslide susceptibility (Mathew et al. 2009).

The quantitative-qualitative relationship between AUC and prediction accuracy can be given as follows: 0.9–1,

excellent; 0.8–0.9, very good; 0.7–0.8, good; 0.6–0.7, average; and 0.5–0.6, poor (Yesilnacar 2005). The ROC curves were obtained using the validation dataset 30 % (158 landslide locations). The result of the ROC curves test is illustrated in Fig. 13. These curves indicate that the SMCE model (Fig. 13a) has relatively lower prediction performance than the PLR model (Fig. 13b). ROC plot assessment results show that in the susceptibility map using SMCE model, the AUC was 0.7616 and the prediction accuracy was 76.16 %. But in the landslide susceptibility map using PLR model, the AUC was 0.8098 and the prediction accuracy was 80.98 % (Fig. 13b).

#### Seed cell area index

In order to assess the reliability of the landslide susceptibility maps produced by PLR and SMCE models, we used seed cell area index (SCAI). The SCAI method was proposed by Suzen and Doyuran (2004). The logic behind SCAI lies in the correct classification of seed cells within a very conservative areal extent, and it is expected that the high and very high susceptibility classes should have very small SCAI values, and low and very low susceptibility classes will have higher SCAI values (Kincal et al. 2009; Akgun and Turk 2010; Akgun 2012). The landslide susceptibility area percent values are divided by the landslide seed cell percent values to develop the seed cell area index density of landslides among the classes (Table 10). In Table 10, it can be seen that the generated map is accurate because the high and very high susceptibility classes have very low SCAI values, whereas the SCAI values of the very low and low susceptibility classes are very high. This result confirms the result of (Kincal et al. 2009; Akgun and Turk 2010; Akgun 2012) as the SCAI value should decrease from low to very high susceptibility zones.

#### Conclusion

Over the last three decades, the regional landslide susceptibility assessment has been one of the hot topics in the international landslide literature because this assessment is a difficult and non-linear problem. The main goal of the current study was to produce landslide susceptibility mapping by probabilistic

**Table 10** Distribution of landslide susceptibility zones in landslides and seed cells for PLR and SMCE models

Landslide susceptibility classes	Percentage in total area		Percentage in seed cells		Seed cell area index	
	PLR	SMCE	PLR	SMCE	PLR	SMCE
Low	7.27	2.45	1.27	0.63	5.74	3.87
Moderate	20.62	4.27	13.92	1.27	1.48	3.37
High	41.37	11.52	39.24	3.80	1.05	3.03
Very high	30.74	81.76	44.94	94.30	0.68	0.87

likelihood ratio (PLR) and spatial multi criteria evaluation (SMCE) models based on GIS in the north of Tehran metropolitan, Iran. Seventeen data layers are exploited to detect the most susceptible areas. These factors are slope degree, slope aspect, altitude, plan curvature, profile curvature, surface area ratio (SAR), topographic position index (TPI), topographic wetness index (TWI), stream power index (SPI), slope length (LS), lithology, land use, normalized difference vegetation index (NDVI), distance from faults, distance from rivers, distance from roads, and drainage density. Finally, the two landslide susceptibility maps were validated using receiver operating characteristic (ROC) curves and SCAI. The validation results show that the probabilistic likelihood ratio model has slightly better predication rate accuracy (80.98 %) which is better than the spatial multi-criteria evaluation (76.16 %) model. Also, reliability of the landslide susceptibility maps produced by seed cell area index was confirmed in the study area. The main characteristic of SMCE method is that there are no rules in designing and organizing the criteria tree, in the assignment of the weights, or in the normalization process. In fact, defining the value functions is one of the major discussion topics in the multi-criteria evaluation procedure. However, SMCE is a very flexible tool that can be applied in many cases with very different data sets, even in poor data conditions; it is also a weakness for the mentioned approach. Because of it, it is up to the assessor teams to define whether or not all relevant criteria are included in the assessment. So, the results obtained in the research showed that the frequency ratio and spatial multi-criteria evaluation models have a reasonably satisfactory performance. However, in landslide susceptibility mapping, hazard risk estimation, and assessment of its performance, the main step is quality of the available data, and it depends not only on the methodology followed.

These landslide susceptibility maps can be used for optimum management by decision makers and land use planners, and also avoidance of susceptible regions in study area. Also, it is worth mentioning that the similar method can be used elsewhere in Iran where the same geological and topographical feature prevails.

**Acknowledgments** The authors gratefully acknowledge the National Geographic Organization (NGO-Iran) (<http://www.ngo-iran.ir/ngo.htm>) for providing the IRS satellite images. This research was carried out as part of the first author's PhD thesis at the watershed management engineering, Tarbiat Modares University, Mazandaran, Iran. Also, the authors would like to thank two anonymous reviewers for their helpful comments on the previous version of the manuscript.

## References

- Akgun A (2012) A comparison of landslide susceptibility maps produced by logistic regression, multi-criteria decision, and likelihood ratio methods: a case study at İzmir, Turkey. *Landslides* 9:93–106
- Akgun A, Sezer EA, Nefeslioglu HA, Gokceoglu C, Pradhan B (2012) An easy-to-use MATLAB program (MamLand) for the assessment of landslide susceptibility using a Mamdani fuzzy algorithm. *Comput Geosci* 38(1):23–34
- Akgun A, Turk N (2010) Landslide susceptibility mapping for Ayvalik (Western Turkey) and its vicinity by multi criteria decision analysis. *Environ Earth Sci* 61:595–611
- Aleotti P, Chowdhury R (1999) Landslide hazard assessment: summary review and new perspectives. *Bull Eng Geol Environ* 58:21–44
- Althuwaynee OF, Pradhan B, Lee S (2012) Application of an evidential belief function model in landslide susceptibility mapping. *Comput Geosci* 44:120–135. doi:10.1016/j.cageo.2012.3
- Aniya M (1985) Landslide-susceptibility mapping in the Amahata river basin, Japan. *Annals Associ of American Geograph* 75(1):102–114
- Atkinson PM, Massari R (2011) Autologistic modelling of susceptibility to landsliding in the Central Apennines, Italy. *Geomorphology* 130(1–2):55–64
- Ayalew L, Yamagishi H (2005) The application of GIS-based logistic regression for landslide susceptibility mapping in the Kakuda-Yahiko Mountains, Central Japan. *Geomorphology* 65(1–2):15–31
- Ayalew L, Yamagishi H, Ugawa N (2004) Landslide susceptibility mapping using GIS based weighted linear combination, the case in Tsugawa area of Agano River, Niigata Prefecture, Japan. *Landslides* 1(1):73–81
- Ballabio C, Sterlacchini S (2012) Support vector machines for landslide susceptibility mapping: the Staffora River Basin case study, Italy. *Math Geosci* 44:47–70
- Bednarik M, Magulova B, Matys M, Marschalko M (2010) Landslide susceptibility assessment of the Kralovany–Liptovsky Mikulas railway case study. *Phys Chem Earth Parts A/B/C* 35(3–5):162–171
- Beven K, Kirkby MJ (1979) A physically based, variable contributing area model of basin hydrology. *Hydrol Sci Bull* 24:43–69
- Binaghi E, Luzi L, Madella P, Pergalani F, Rampini A (1998) Slope instability zonation: a comparison between certainty factor and Fuzzy Dempster–Shafer approaches. *Nat Hazards* 17:77–97
- Boerboom L, Flacke J, Sharifi A, Alan O (2009) Web-based spatial multi-criteria evaluation (SMCE) software, ITC Working paper 1, for the ForestClim Project 25 pp
- Castellanos E, Van Westen CJ (2007) Generation of a landslide risk index map for Cuba using spatial multi-criteria evaluation. *Landslide* 4:311–325
- Cevik E, Topal T (2003) GIS-based landslide susceptibility mapping for a problematic segment of the natural gas pipeline, Hendek (Turkey). *Environ Geol* 44(8):949–962
- Champati Ray DP, Dimri S, Lakhera RC, Sati S (2007) Fuzzy-based method for landslide hazard assessment in active seismic zone of Himalaya. *Landslides* 4:101–111
- Choi J, Oh HJ, Lee HJ, Lee C, Lee S (2012) Combining landslide susceptibility maps obtained from frequency ratio, logistic regression, and artificial neural network models using ASTER images and GIS. *Eng Geol* 124:12–23
- Chung CJ, Fabbri AG (2003) Validation of spatial prediction models for landslide hazard mapping. *Nat Hazards* 30:451–472
- Constantin M, Bednarik M, Jurchescu MC, Vlaicu M (2011) Landslide susceptibility assessment using the bivariate statistical analysis and the index of entropy in the Sibiciu Basin (Romania). *Environ Earth Sci* 63:397–406
- Costanzo D, Rotigliano E, Irigaray C, Jimenez-Pervarez JD, Chacon J (2012) Factors selection in landslide susceptibility modelling on large scale following the gis matrix method: application to the river Beiro basin (Spain). *Nat Hazards Earth Syst Sci* 12:327–340
- Dai FC, Lee CF (2001) Terrain-based mapping of landslide susceptibility using a geographical information system: a case study. *Canadian Geotechn J* 38(5):911–923

- Devkota KC, Regmi AD, Pourghasemi HR, Yoshida K, Pradhan B, Ryu IC, Dhital MR, Althuwaynee OF (2012) Landslide susceptibility mapping using certainty factor, index of entropy and logistic regression models in GIS and their comparison at Mugling-Narayanghat road section in Nepal Himalaya. *Nat Hazards*. doi:10.1007/s11069-012-0347-6
- Dietrich EW, Reiss R, Hsu ML, Montgomery DR (1995) A process-based model for colluvial soil depth and shallow landsliding using digital elevation data. *Hydrol Processes* 9:383–400
- Ercanoglu M, Gokceoglu C (2002) Assessment of landslide susceptibility for a landslide-prone area (North of Yenice, NW Turkey) by fuzzy approach. *Environ Geol* 41:720–730
- Ercanoglu M, Gokceoglu C (2004) Use of fuzzy relations to produce landslide susceptibility map of a landslide prone area (West Black Sea Region, Turkey). *Eng Geol* 75:229–250
- Ercanoglu M, Kasmer O, Temiz N (2008) Adaptation and comparison of expert opinion to analytical hierarchy process for landslide susceptibility mapping. *Bull Eng Geol Environ* 67:565–578
- Ermini L, Catani F, Casagli N (2005) Artificial neural networks applied to landslide susceptibility assessment. *Geomorphology* 66:327–343
- Felicísimo A, Cuartero A, Remondo J, Quiros E (2012) Mapping landslide susceptibility with logistic regression, multiple adaptive regression splines, classification and regression trees, and maximum entropy methods: a comparative study. *Landslides*. doi:10.1007/s10346-012-0320-1
- Geology Survey of Iran (GSI) (1997) [http://www.gsi.ir/Main/Lang\\_en/index.html](http://www.gsi.ir/Main/Lang_en/index.html)
- Gokceoglu C, Sezer EA (2012) Soft computing modeling in landslide susceptibility assessment. In: Pradhan B, Buchroithner M (eds) *Terrigenous mass movements*. Springer, Berlin, pp 51–90. doi:10.1007/978-3-642-25495-6-2
- Gokceoglu C, Sonmez H, Ercanoglu M (2000) Discontinuity controlled probabilistic slope failure risk maps of the Altindag (settlement) region in Turkey. *Eng Geol* 55:277–296
- Gomez H, Kavzoglu T (2005) Assessment of shallow landslide susceptibility using artificial neural networks in Jabonosa River Basin, Venezuela. *Eng Geol* 78:11–27
- Gorsevski PV, Jankowski P (2008) Discreting landslide susceptibility using rough sets. *Comput Environ Urban Syst* 32:53–65
- Gorsevski PV, Jankowski P, Paul PE (2006) Heuristic approach for mapping landslide hazard integrating fuzzy logic with analytic hierarchy process. *Control Cybern* 35(1):1–26
- Guzzetti F, Carrara A, Cardinali M, Reichenbach P (1999) Landslide hazard evaluation: a review of current techniques and their application in a multi-scale study, Central Italy. *Geomorphology* 31:81–216
- Hasekiogullari GD, Ercanoglu M (2012) A new approach to use AHP in landslide susceptibility mapping: a case study at Yenice (Karabuk, NW Turkey). *Nat Hazards*. doi:10.1007/s11069-012-0218-1
- He S, Pan P, Dai L, Wang H, Liu J (2012) Application of kernel-based Fisher discriminant analysis to map landslide susceptibility in the Qinggan River delta, Three Gorges, China. *Geomorphology* 171–172:30–41
- Hengl T, Gruber S, Shrestha DP (2003) Digital terrain analysis in ILWIS. International Institute for Geo-Information Science and Earth Observation Enschede, The Netherlands, p 62
- Herwijnen MV (1999) Spatial decision support for environmental management. *Vrije Universiteit, Amsterdam*, 274
- Hizbaron DR, Baiquni M, Sartohadi J, Rijanta R, Coy M (2011) Assessing social vulnerability to seismic hazard through spatial multi criteria evaluation in Bantul District, Indonesia. *Conference of Development on the Margin, Tropentag 2011*, 4 pp
- Irigaray C, Fernandez T, Hamdouni REI, Chacon J (2007) Evaluation and validation of landslide-susceptibility maps obtained by a GIS matrix method: examples from the Betic Cordillera (southern Spain). *Nat Hazards* 41:61–79
- I.R. of Iran Meteorological Org (IRIMO) (2011) <http://www.irimo.ir/english>
- Jenness J (2002) Surface Areas and Ratios from Elevation Grid, Jenness Enterprises, [http://www.jennessent.com/arcview/surface\\_areas.htm](http://www.jennessent.com/arcview/surface_areas.htm) (connected: 10.08.2003)
- Juang CH, Lee DH, Sheu C (1992) Mapping slope failure potential using fuzzy sets. *J Geotech Eng Div ASCE* 118:475–493
- Kanungo DP, Arora MK, Sarkar S, Gupta RP (2006) A comparative study of conventional, ANN black box, fuzzy and combined neural and fuzzy weighting procedures for landslide susceptibility zonation in Darjeeling Himalayas. *Eng Geol* 85:347–366
- Kincal C, Akgun A, Koca MY (2009) Landslide susceptibility assessment in the Izmir (West Anatolia, Turkey) city center and its near vicinity by the logistic regression method. *Environ Earth Sci* 59:745–756
- Komac M (2006) A landslide susceptibility model using analytical hierarchy process method and multivariate statistics in perialpine Slovenia. *Geomorphology* 74:17–28
- Kritikos T, Davies TRH (2011) GIS-based multi-criteria decision analysis for landslide susceptibility mapping at northern Evia, Greece. *Z dt Ges Geowiss* 162(4):421–434
- Lee S (2004) Soil erosion assessment and its verification using the universal soil loss equation and geographic information system: a case study at Boun, Korea. *Environ Geol* 45(4):457–465
- Lee S, Choi J, Oh H (2009) Landslide susceptibility mapping using a neuro-fuzzy. Abstract presented at American Geophysical Union, Fall Meeting 2009, abstract #NH53A-1075
- Lee S, Min K (2001) Statistical analysis of landslide susceptibility at Yongin, Korea. *Environ Geol* 40:1095–1113
- Lee S, Pradhan B (2006) Probabilistic landslide risk mapping at Penang Island, Malaysia. *J Earth Syst Sci* 115(6):661–672
- Lee S, Pradhan B (2007) Landslide hazard mapping at Selangor, Malaysia using frequency ratio and logistic regression models. *Landslides* 4:33–41
- Lee S, Ryu JH, Kim IS (2007) Landslide susceptibility analysis and its verification using likelihood ratio, logistic regression, and artificial neural network models: case study of Youngin, Korea. *Landslides* 4:327–338
- Lee S, Talib JA (2005) Probabilistic landslide susceptibility and factor effect analysis. *Environ Geol* 47:982–990
- Li C, Ma T, Sun L, Li W, Zheng A (2011) Application and Verification of fractal approach to landslide susceptibility mapping. *Natl Hazards*. doi:10.1007/s11069-011-9804-x
- Looijen JM (2010) EIA & SEA: Environmental Impact Assessment and Strategic Environmental Assessment using spatial decision support tools: distance education. ITC, Enschede, 2010
- Malczewski J (1999) GIS and multi criteria decision analysis. Wiley, New York, p 408. ISBN 978-0-471-32944-2
- Marjanović M, Kovačević M, Bajat B, Voženilek V (2011) Landslide susceptibility assessment using SVM machine learning algorithm. *Eng Geol* 123:225–234
- Mathew J, Jha VK, Rawat GS (2009) Landslide susceptibility zonation mapping and its validation in part of Garhwal Lesser Himalaya, India, using binary logistic regression analysis and receiver operating characteristic curve method. *Landslides* 6:17–26
- Melchiorre C, Matteucci M, Azzoni A, Zanchi A (2008) Artificial neural networks and cluster analysis in landslide susceptibility zonation. *Geomorphology* 94:379–400
- Mohammady M, Pourghasemi HR, Pradhan B (2012) Landslide susceptibility mapping at Golestan Province Iran: a comparison between frequency ratio, Dempster-Shafer, and weights-of-evidence models. *J Asian Earth Sci* 61:221–236
- Moore ID, Burch GJ (1986) Sediment transport capacity of sheet and rill flow: application of unit stream power theory. *Water Res* 22:1350–1360
- Moore ID, Grayson RB, Ladson AR (1991) Digital terrain modeling: a review of hydrological, geomorphological, and biological applications. *Hydro Process* 5:3–30



- Nafouti MH, Chabok Boldaje M (2011) Spatial prioritizing of pastures using spatial multi criteria evaluation (Case study: Yoosef Abad watershed—Iran). 2011 2nd International Conference on Environmental Engineering and Applications IPCBEE vol. 17 (2011) IACSIT Press, Singapore, p. 4
- Nagarajan R, Roy A, Vinod Kumar R, Mukherjee A, Khire MV (2000) Landslide hazard susceptibility mapping based on terrain and climatic factors for tropical monsoon regions. *Bull Eng Geol Env* 58:275–287
- Nandi A, Shakoor A (2010) A GIS-based landslide susceptibility evaluation using bivariate and multivariate statistical analyses. *Eng Geol* 110:11–20
- Nefeslioglu HA, Gokceoglu C, Sonmez H (2008) An assessment on the use of logistic regression and artificial neural networks with different sampling strategies for the preparation of landslide susceptibility maps. *Eng Geol* 97:171–191
- Nefeslioglu, H.A., Sezer, E., Gökçeoğlu, C., Bozkır, A.S., Duman, T.Y (2010) Assessment of landslide susceptibility by decision trees in the metropolitan area of Istanbul, Turkey. *Mathematical Problems in Engineering*, 2010, Article ID: 901095
- Negnevitsky M (2002) *Artificial intelligence—a guide to intelligent systems*. Addison-Wesley Co, Great Britain
- Nilaweera NS, Notalaya P (1999) Role of tree roots in slope stabilisation. *Bull Eng Geol Environ* 57:337–342
- Oh HJ, Lee S (2010) Cross-validation of logistic regression model for landslide susceptibility mapping at Geneoung areas, Korea. *Disaster Adv* 3(2):44–55
- Oh HJ, Lee S (2011) Cross-application used to validate landslide susceptibility maps using a probabilistic model from Korea. *Environ Earth Sci* 64(2):395–409
- Oh HJ, Pradhan B (2011) Application of a neuro-fuzzy model to landslide-susceptibility mapping for shallow landslides in a tropical hilly area. *Comput Geosci* 37(9):1264–1276. doi:10.1016/j.cageo.2010.10.012
- Okimura T, Kawatani T (1987) Mapping of the potential surface—failure sites on granite slopes. In: Gardiner E (ed) *International geomorphology 1986 part I*. Wiley, Chichester, pp 121–138
- Ozdemir A (2009) Landslide susceptibility mapping of vicinity of Yaka Landslide (Gelendost, Turkey) using conditional probability approach in GIS. *Environ Geol* 57:1675–1686
- Pachauri AK, Gupta PV, Chander R (1998) Landslide zoning in a part of the Garhwal Himalayas. *Environ Geol* 36(3–4):325–334
- Pachauri AK, Pant M (1992) Landslide hazard mapping based on geological attributes. *Eng Geol* 32:81–100
- Parise M (2001) Landslide mapping techniques and their use in the assessment of the landslide hazard. *Phys Chem Earth* 26(9):697–703
- Piegari E, Cataudella V, Di Maio R, Milano L, Nicodemi M, Soldovieri MG (2009) Electrical resistivity tomography and statistical analysis in landslide modelling: a conceptual approach. *J Appl Geophysics* 68(2):151–158
- Pielke RA, Schellnhuber HJ, Sahagian D (2003) Non-linearities in the earth system. *Global Change News Lett* 55:11–15
- Pourghasemi HR (2008) Landslide hazard assessment using fuzzy logic (Case study: a part of Haraz Watershed). A thesis presented for M.Sc. degree in Watershed Management, Faculty of Natural Resources, Department of Watershed Management, Tarbiat Modarres University, Iran (in Persian).
- Pourghasemi HR, Pradhan B, Gokceoglu C, Mohammadi M, Moradi HR (2012a) Application of weights-of-evidence and certainty factor models and their comparison in landslide susceptibility mapping at Haraz watershed, Iran. *Arab J Geosci*. doi:10.1007/s12517-012-0532-7
- Pourghasemi HR, Pradhan B, Gokceoglu C, Deylami Moezzi K (2012b) A comparative assessment of prediction capabilities of Dempster-Shafer and weights-of-evidence models in landslide susceptibility mapping using GIS. *Geomatics Nat Hazards Risk*. doi:10.1080/19475705.2012.662915
- Pourghasemi HR, Mohammady M, Pradhan B (2012c) Landslide susceptibility mapping using index of entropy and conditional probability models in GIS: Safarood Basin, Iran. *Catena* 97:71–84. doi:10.1016/j.catena.2012.05.005
- Pourghasemi HR, Pradhan B, Gokceoglu C (2012d) Application of fuzzy logic and analytical hierarchy process (AHP) to landslide susceptibility mapping at Haraz watershed, Iran. *Nat Hazards*. doi:10.1007/s11069-012-0217-2
- Pourghasemi HR, Gokceoglu C, Pradhan B, Deylami Moezzi K (2012e) Landslide susceptibility mapping using a spatial multi criteria evaluation model at Haraz Watershed, Iran. In: Buchroithner M, Pradhan B (eds) *Terrigenous mass movements*. Springer, Berlin, pp 23–49. doi:10.1007/978-3-642-25495-6-2
- Pourghasemi HR, Goli Jirandeh A, Pradhan B, Xu C, Gokceoglu C (2012) Landslide susceptibility mapping using support vector machine and GIS, *J Earth Syst Sci* (in press)
- Pourghasemi HR, Pradhan B, Gokceoglu C (2012g) Remote sensing data derived parameters and its use in landslide susceptibility assessment using Shannon's entropy and GIS. *Appl Mech Mater* 225:486–491. doi:10.4028/www.scientific.net/AMM.225.486
- Pradhan B (2010a) Remote sensing and GIS-based landslide hazard analysis and cross validation using multivariate logistic regression model on three test areas in Malaysia. *Adv Space Res* 45:1244–1256
- Pradhan B (2010b) Application of an advanced fuzzy logic model for landslide susceptibility analysis. *Int J Comput Intell Syst* 3:370–381
- Pradhan B (2010c) Landslide susceptibility mapping of a catchment area using frequency ratio, fuzzy logic and multivariate logistic regression approaches. *J Indian Soc Remote Sens* 38(2):301–320
- Pradhan B (2011a) Manifestation of an advanced fuzzy logic model coupled with geoinformation techniques for landslide susceptibility analysis. *Environ Ecol Stat* 18(3):471–493. doi:10.1007/s10651-010-0147-7
- Pradhan B (2011b) Use of GIS-based fuzzy logic relations and its cross application to produce landslide susceptibility maps in three test areas in Malaysia. *Environ Earth Sci* 63(2):329–349
- Pradhan B (2011c) An assessment of the use of an advanced neural network model with five different training strategies for the preparation of landslide susceptibility maps. *J Data Sci* 9(1):65–81
- Pradhan B (2012) A comparative study on the predictive ability of the decision tree, support vector machine and neuro-fuzzy models in landslide susceptibility mapping using GIS. *Comput & Geosci*, doi:10.1016/j.cageo.2012.08.023
- Pradhan B, Sezer EA, Gokceoglu C, Buchroithner MF (2010a) Landslide susceptibility mapping by neuro-fuzzy approach in a landslide prone area (Cameron Highland, Malaysia). *IEEE Trans Geosci Remote Sens* 48(12):4164–4177
- Pradhan B, Lee S (2007) Utilization of optical remote sensing data and GIS tools for regional landslide hazard analysis by using an artificial neural network model. *Earth Sci Front* 14(6):143–152
- Pradhan B, Lee S, Buchroithner MF (2009) Use of geospatial data for the development of fuzzy algebraic operators to landslide hazard mapping: a case study in Malaysia. *Appl Geomatics* 1:3–15
- Pradhan B, Lee S, Mansor S, Buchroithner MF, Jallaluddin N, Khujaimah Z (2008) Utilization of optical remote sensing data and geographic information system tools for regional landslide hazard analysis by using binomial logistic regression model. *Appl Remote Sens* 2:1–11
- Pradhan B, Mansor S, Pirasteh S, Buchroithner M (2011) Landslide hazard and risk analyses at a landslide prone catchment area using statistical based geospatial model. *Int J Remote Sens* 32(14):4075–4087. doi:10.1080/01431161.2010.484433
- Pradhan B, Pirasteh S (2010) Comparison between prediction capabilities of neural network and fuzzy logic techniques for landslide susceptibility mapping. *Disaster Adv* 3(2):26–34
- Pradhan B, Youssef AM, Varathrajoo R (2010b) Approaches for delineating landslide hazard areas using different training sites in an advanced artificial neural network model. *Geo-Spat Inf Sci* 13(2):93–102

- Rahman Md R, Saha SK (2008) Remote sensing, spatial multi criteria evaluation (SMCE) and analytical hierarchy process (AHP) in optimal cropping pattern planning for a flood prone area. *J Spatial Sci* 53:2161–177
- Remondo J, Gonzalez A, Diaz De Teran JR, Cendrero A, Fabbri A, Cheng CF (2003) Validation of landslide susceptibility maps: examples and applications from a case study in Northern Spain. *Nat Hazards* 30(3):437–449
- Saaty T (1980) *The analytical hierarchy Process*. McGraw-Hill, New York
- Sarkar S, Kanungo DP (2004) An integrated approach for landslide susceptibility mapping using remote sensing and GIS. *Photogramm Eng Remote Sens* 70(5):617–625
- Sezer EA, Pradhan B, Gokceoglu C (2011) Manifestation of an adaptive neuro-fuzzy model on landslide susceptibility mapping: Klang valley, Malaysia. *Expert Syst Appl* 38(7):8208–8219
- Sharifi MA, Retsios V (2004) Site selection for waste disposal through spatial multiple criteria decision analysis. *J Telecommun Inf Technol* 3:1–11
- Sidle RC, Ochiai H (2006) Landslides: process, prediction, and land use. *Water Resour Monogr Ser* 18:312. doi:10.1029/WM018
- Song Y, Gong J, Gao S, Wang D, Cui T, Li Y, Wei B (2012a) Susceptibility assessment of earthquake-induced landslides using Bayesian network: a case study in Beichuan, China. *Comput Geosci* 42:189–199
- Song KY, Oh JJ, Choi J, Park I, Lee C, Lee S (2012b) Prediction of landslides using ASTER imagery and data mining models. *Adv Space Res* 49:978–993
- Suzen ML, Doyuran V (2004) A comparison of the GIS based landslide susceptibility assessment methods: multivariate versus bivariate. *Environ Geol* 45:665–679
- Swets JA (1988) Measuring the accuracy of diagnostic systems. *Science* 240:1285–1293
- Tagil S, Jenness J (2008) GIS-based automated landform classification and topographic, land cover and geologic attributes of landforms around the Yazoren Poje, Turkey. *J Appl Sci* 8(6):910–921
- Talebi A, Uijlenhoet R, Troch PA (2007) Soil moisture storage and hillslope stability. *Nat Hazards Earth Syst Sci* 7:523–534
- Tangestani MH (2009) A comparative study of Demster-Shafer and fuzzy models for landslide susceptibility mapping using a GIS: an experience from Zagros Mountains, SW Iran. *J Asian Earth Sci* 35:66–73
- Terlien MTJ, Van Asch TWJ, Van Westen CJ (1995) Deterministic modelling in GIS-based landslide hazard assessment. In: Carrar A, Guzzetti F (eds) *Geographical information systems in assessing natural hazards*. Kluwer, London, pp 57–77
- Tien Bui D, Pradhan B, Lofman O, Revhaug I (2012a) Landslide susceptibility assessment in Vietnam using support vector machines, decision tree and Naive Bayes models. *Math Probl Eng* 2012:1–26. doi:10.1155/2012/974638
- Tien Bui D, Pradhan B, Lofman O, Revhaug I, Dick OB (2011) Landslide susceptibility mapping at Hoa Binh province (Vietnam) using an adaptive neuro fuzzy inference system and GIS. *Comput Geosci* (Article on-line first available). doi:10.1016/j.cageo.2011.10.031
- Tien Bui D, Pradhan B, Lofman O, Revhaug I, Dick OB (2012b) Landslide susceptibility assessment in the Hoa Binh province of Vietnam using artificial neural network. *Geomorphology*. doi:10.1016/j.geomorph.2012.04.023, Article online first available
- Tien Bui D, Pradhan B, Lofman O, Revhaug I, Dick OB (2012c) Spatial prediction of landslide hazards in Vietnam: a comparative assessment of the efficacy of evidential belief functions and fuzzy logic models. *Catena* 96:28–40
- Vahidnia MH, Alesheikh AA, Alimohammadi A, Hosseinali F (2010) A GIS-based neuro-fuzzy procedure for integrating knowledge and data in landslide susceptibility mapping. *Comput Geosci* 36:1101–1114
- Varnes DJ (1978) Slope movement types and processes. In: Schuster RL, Krizek RJ (eds) *Landslides analysis and control*. Special report, vol. 176. Transportation Research Board, National Academy of Sciences, New York, pp. 11–33
- Varnes DJ (1984) With IAEG Commission on Landslides and Other Mass Movements: landslide hazard zonations: a review of principles and practices. UNESCO, Paris, p 63
- Van Westen CJ (2012) Living with landslide risk in Europe: assessment, effects of global change, and risk management strategies, 7th Framework Program Cooperation Theme 6 Environment (including climate change) Sub-Activity 6.1.3 Natural Hazards, GIS-based training package on landslide risk assessment Work Package 7–Dissemination of project results, pp. 133
- Wan S (2012) Entropy-based particle swarm optimization with clustering analysis on landslide susceptibility mapping. *Environ Earth Sci*. doi:10.1007/s12665-012-1832-7
- Wang HB, Wu SR, Shi JS, Li B (2011) Qualitative hazard and risk assessment of landslides: a practical framework for a case study in China. *Nat Hazards*. doi:10.1007/s11069-011-0008-1
- Xu C, Dai F, Xu X, Lee YH (2012) GIS-based support vector machine modeling of earthquake-triggered landslide susceptibility in the Jianjiang River watershed. *China Geomorphol*. doi:10.1016/j.geomorph.2011.12.040
- Yalcin A (2005) An investigation on Ardesen (Rize) region on the basis of landslide susceptibility, KTU, PhD Thesis (in Turkish)
- Yalcin A (2008) GIS-based landslide susceptibility mapping using analytical hierarchy process and bivariate statistics in Ardesen (Turkey): comparisons of results and confirmations. *Catena* 72:1–12
- Yalcin A, Reis S, Aydinoglu AC, Yomralioglu T (2011) A GIS-based comparative study of frequency ratio, analytical hierarchy process, bivariate statistics and logistics regression methods for landslide susceptibility mapping in Trabzon, NE Turkey. *Catena* 85(3):274–287
- Yao X, Tham LG, Dai FC (2008) Landslide susceptibility mapping based on support vector machine: a case study on natural slopes of Hong Kong, China. *Geomorphology* 101:572–582
- Yeon YK, Han JG, Ryu KH (2012) Landslide susceptibility mapping in Injae, Korea, using a decision tree. *Eng Geol* 116:274–283
- Yesilnacar E, Topal T (2005) Landslide susceptibility mapping: a comparison of logistic regression and neural networks methods in a medium scale study, Hendek region (Turkey). *Eng Geol* 79:251–266
- Yesilnacar EK (2005) The application of computational intelligence to landslide susceptibility mapping in Turkey, Ph.D Thesis. Department of Geomatics the University of Melbourne, pp 423.
- Yilmaz I (2009a) A case study from Koyulhisar (Sivas-Turkey) for landslide susceptibility mapping by artificial neural networks. *Bull Eng Geol Environ* 68:297–306
- Yilmaz I (2009b) Landslide susceptibility mapping using frequency ratio, logistic regression, artificial neural networks and their comparison: a case study from Kat landslides (Tokat-Turkey). *Comput Geosci* 35:1125–1138
- Yilmaz I (2010) Comparison of landslide susceptibility mapping methodologies for Koyulhisar, Turkey: conditional probability, logistic regression, artificial neural networks, and support vector machine. *Environ Earth Sci* 61:821–836
- Yilmaz C, Topal T, Suzen ML (2012) GIS-based landslide susceptibility mapping using bivariate statistical analysis in Devrek (Zonguldak-Turkey). *Environ Earth Sci* 65:2161–2178
- Zare M, Pourghasemi HR, Vafakhah M, Pradhan B (2012) Landslide susceptibility mapping at Vaz watershed (Iran) using an artificial neural network model: a comparison between multi-layer perceptron (MLP) and radial basic function (RBF) algorithms. *Arab J Geosci*. doi:10.1007/s12517-012-0610-x